Thermodynamics of Membrane Receptors and Channels

Edited by
Meyer B. Jackson, Ph.D.
Professor
Department of Physiology
University of Wisconsin-Madison Medical School
Madison, Wisconsin

CRC Press
Boca Raton Ann Arbor London Tokyo

Chapter 5

MOLECULAR CROWDING AND PROTEIN ORGANIZATION IN BIOLOGICAL MEMBRANES

James R. Abney and Bethe A. Scalettar

TABLE OF CONTENTS

0-8493-6908-8/93/$0.00+$.50

I. INTRODUCTION

Lateral heterogeneity in the distribution of membrane proteins is a prominent structural feature of biological membranes that is essential for many aspects of membrane function.[1,2] For example, facilitated transport is coupled to differences in protein composition between the apical and basolateral surfaces of epithelial cells;[3] synaptic transmission is dependent on the aggregation of AChR at the neuromuscular junction;[4,5] and action potential propagation in myelinated nerve fibers is facilitated by the collection of ion channels at nodes of Ranvier.[6] Since heterogeneity in protein distribution is so important and ubiquitous, considerable effort has been directed at identifying the forces that act to maintain it. Certain aspects of this topic will be the focus of this chapter.

It has been well established in the literature that specific biological mechanisms often act to regulate protein organization. These mechanisms include attachment of protein to the cytoskeleton, confinement of protein to domains created by the cytoskeleton and tight junctions, and interactions of proteins with molecules in the extracellular matrix and in the membranes of adjacent cells. These same factors play a role in determining protein (and lipid) mobility as well.[3,7-14]

For systems in which protein concentrations are high, such as biological membranes, nonspecific (e.g., electrostatic) interprotein interactions can also play a role in dictating organization, although this fact is sometimes overlooked.

For example, if protein molecules attract, they will tend to aggregate, and their distribution will become more heterogeneous. Conversely, if protein molecules repel, they will tend to disperse, and their distribution will become more homogeneous. These qualitative arguments can be made quantitative and the results used to deepen our understanding of membrane behavior.

In this chapter, we establish a quantitative connection between *nonspecific* protein-protein interactions and protein organization. In general, the systems under consideration will be simple, consisting of lipid and one species of protein present at high concentration. Analysis of such simple systems illustrates the important physical principles underlying protein organization and provides a foundation upon which to formulate descriptions of organization in complex biological membranes. We begin by discussing the origins of nonspecific protein-protein interactions. We then introduce formulae from fluid theory that relate the short range organization of membrane proteins to nonspecific interprotein interactions. The utility of the fluid theoretic relationships will be illustrated by showing how they can be used to measure the real forces between proteins in membranes and to compute thermodynamic and kinetic properties of the membrane. We conclude by considering the effects that protein-protein interactions have on long range organization in membranes.

II. ORIGINS OF PROTEIN-PROTEIN INTERACTIONS

Although the relevant data are somewhat lacking, it appears likely that proteins in membranes interact much as do proteins in aqueous solution. In this section, we briefly describe three relatively nonspecific mechanisms through which membrane proteins *might* interact: excluded-volume, electrostatic, and lipid-mediated. The first two mechanisms arise in descriptions of interprotein interactions in three-dimensional aqueous solutions; the last does not.

A relatively simple description of interprotein interactions will be adopted. Specifically, we will focus on a two-dimensional planar projection of the membrane. It will be assumed that a "central-force" description is applicable, i.e., that the energy of interaction between two proteins depends only on their center-to-center separation, r, in the plane and not on their relative orientation. Thus, the interactions studied will have no angular dependence or, alternatively, the angular dependence will be averaged over by integration. In this simplified picture, the pair potential describing the interaction between two proteins can be denoted $u(r)$. The associated pair force, $f(r)$, can be found by differentiation:

$$f(r) = -\frac{du(r)}{dr} \tag{1}$$

In addition, it will be assumed (unless otherwise noted) that the total interaction energy of a system of N proteins, U_N, is "pairwise additive," i.e., that the total

potential is simply the pairwise sum of the interaction potentials between each pair of neighbors. Hence,

$$U_N = \sum_{i<j} u(r_{ij}) \tag{2}$$

where r_{ij} denotes the separation between the ith and jth proteins. An analogous expression is obeyed by the pair force. It is also assumed that the various interactions, e.g., excluded-volume, electrostatic, and lipid-mediated, between a pair of proteins are pairwise additive. The origins and significance of pairwise additivity will be considered in more detail in subsequent sections.

Of course, at a detailed level, the interactions between membrane proteins will depend on the particular proteins and lipids under consideration. Moreover, in certain cases, such as dimerization or crystallization, very specific short range attractions, including hydrogen bonds, salt bridges, and covalent interactions, may play an important role in dictating behavior.[15] However, to capture the essence of the relationship between interactions and organization, we need explicitly to discuss only "generic" interactions and can suppress reference to very specific types of interprotein interactions. Such an approach has been shown to reveal many of the important features of other membrane phenomena, including lipid-protein interactions[16] and protein diffusion.[14] We now turn attention to characterizing these generic interactions.

A. Excluded-Volume Interactions

The most basic interaction between proteins arises from their finite volume: proteins can approach one another to contact, but they cannot overlap. This excluded-volume interaction can be written as

$$u(r) = \begin{cases} \infty & r \le d \\ 0 & r > d \end{cases} \tag{3}$$

where d is the separation between the proteins at contact. The excluded-volume interaction is clearly short range, yet it can profoundly affect the activity,[17] mobility,[14] and long range organization of proteins within the membrane. Because of its simple functional form and ubiquitous nature, the excluded-volume interaction is the most widely used interaction in studies of the relationship between protein-protein forces and protein organization and mobility.

B. Electrostatic Interactions

Electrostatic interactions, which probably dominate the protein-protein force at long range, arise from interactions among charged amino acid residues on each protein. The magnitude and functional form of the electrostatic interaction are determined by the number and location of these charges, as well as the physical properties of the intervening environment. For "typical" membrane proteins that

span the bilayer, charge may be located in a variety of environments: the cytoplasm, the membrane, and the extracellular space. It is, therefore, necessary to specify how the functional form for the electrostatic interaction between two residues will depend on their location.

Consider two limiting cases. First, suppose that two residues on two different proteins are each located in an electrolytic medium, such as the cytoplasm or extracellular space. The potential between the two charges is then screened by counterions and can be described by the Debye-Hückel equation,[18,19]

$$u(r) = \frac{q^2}{\varepsilon_a \varepsilon_0 r} \exp(-\kappa r) \tag{4}$$

if one neglects the membrane/water interface. Here q is the charge on each protein, ε_a is the relative permittivity of the aqueous phase, ε_0 is the permittivity of vacuum, and $1/\kappa$ is the Debye length, an ionic strength dependent length constant that determines the range of interaction. In contrast, suppose that the two residues are each located in a low dielectric medium, such as the membrane interior. The potential between two charges is then given by the expression[20]

$$u(r) = \frac{q^2}{\pi \varepsilon_m \varepsilon_0 d} \sum_{k=1}^{\infty} \sin\left(\frac{k\pi l}{d}\right) \sin\left(\frac{k\pi z}{d}\right) K_0\left(\frac{k\pi r}{d}\right) \tag{5}$$

where d is the thickness of the membrane, ε_m is the relative permittivity of the membrane, $(0,0,l)$ and (r,θ,z) are the cylindrical coordinates of the charges, and K_0 is a modified Bessel function. In Equation 5, it is understood that z can assume the value l or $d-l$ and that one membrane/water interface is located at $z=0$. When $r > d$, this potential falls off very rapidly with r. An expression for the interaction of two charges located on opposite sides of the membrane/water interface has not been derived.

In principle, it is not difficult to calculate the total electrostatic interaction energy between two charged proteins: it is simply given by the sum of the interaction energies between each pair of charges the proteins contain (if pairwise additivity holds). For residues in the cytoplasm or extracellular space, Equation 4 is applicable, and for those in the membrane, Equation 5 is applicable. However, in practice, the mathematical form for this total interaction can become very complicated if the parameter describing the separation of the two proteins is taken to be the vector connecting their center-to-center coordinates, as in a central-force description. (This is because the individual charged amino acids on the proteins will not necessarily lie along this vector; see Figure 1.) The total electrostatic interaction can become particularly complicated when the two proteins are close together. In this case, the closest pairs of charges might be expected to dominate the overall interaction, and the interprotein force could be

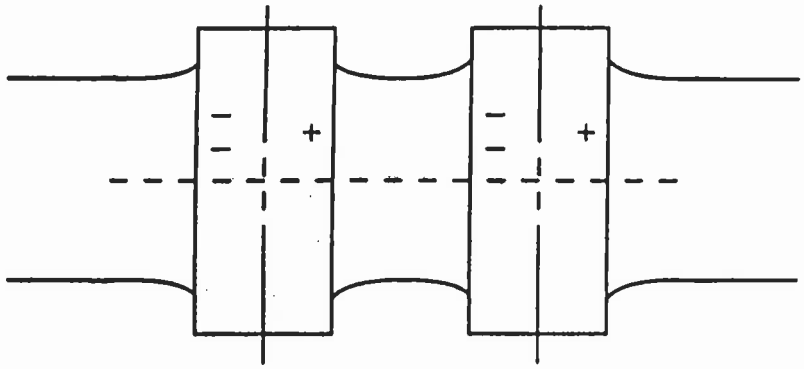

FIGURE 1. Electrostatic protein-protein interactions. Positive and negative charges are indicated by + and –, respectively. The strength of the electrostatic interaction depends on the separation and environment between the charges, as well as the distribution of counterions and charged lipids. Approximate analytical expressions describing the force in two special cases are given in the text. In a central-force description, all forces are assumed to act along the axis (dashed line) separating protein centers. With the particular orientations and separations of charges depicted in the figure, the proteins would probably interact attractively and the force would not be central. However, if the proteins were separated by a large distance and if the force were averaged over orientation (to reflect rotation), the interaction would be central and repulsive since the proteins bear identical total charge. Since it is unlikely that a measured protein-protein force could ever be uniquely fit theoretically, studies of protein-protein interactions have concentrated either on characterizing more unique forms of interaction, such as the lipid-mediated interaction, or on understanding the influence of a given interaction on protein and membrane behavior, independent of the origin of the force.

attractive or repulsive even for proteins whose total charge is identical. (Intuition might lead one to expect that, for like-charged proteins, the interaction must necessarily be repulsive.) Moreover, these short range forces typically will not act precisely along the vector between protein centers and will thus not satisfy the central-force criterion.

However, under certain specialized conditions, the total electrostatic interaction may adopt a relatively simple form. For example, if the protein has a radially symmetric charge distribution, many terms (e.g., the dipole term) in the multipole expansion of the electrostatic potential will vanish. Such proteins will interact through a potential that more nearly approximates a central ($1/r$) potential, like point particles. Moreover, at long range, all proteins may interact like point particles, located at the coordinates given by their centers-of-mass and with total charge given by the sum of their individual charges. If a point-charge approximation is valid, the familiar results will hold: like-charged proteins will interact repulsively, and unlike-charged proteins will interact attractively.

C. Lipid-Mediated Interactions

Another long range contribution to the protein-protein force, the lipid-mediated interaction, may arise to minimize protein-induced perturbation of

adjacent "boundary lipids" (reviewed in Reference 16); see Figure 2. Surprisingly, the source of the perturbation need not be specified, although it is usually thought to arise from conformational changes in the lipid that are required to fit hydrophobic and hydrophilic domains at the lipid/protein interface.[21] In most cases, the lipid-mediated interaction is predicted to be attractive: lipid perturbed by protein is assigned an unfavorable free energy; protein aggregation driven by an attractive lipid-mediated interaction decreases the total amount of this perturbed lipid and, hence, the free energy of the membrane. However, if the induced perturbations differ sufficiently for two unlike proteins, the lipid-mediated interaction can become repulsive. These arguments are similar in style to those invoked in descriptions of surface tension and the hydrophobic effect.

The lipid-mediated protein-protein interaction has been characterized theoretically;[16] however, a functional form for the interaction will not be presented, since it is both complicated and model dependent. Instead, the following qualitative points are noted. First, the interaction is probably not strong: the theories predict a maximum strength of interaction on the order of a few times k_BT or less, where k_B is Boltzmann's constant and T is the temperature. Second, the range of the interaction is predicted to be about twice the distance over which lipids are perturbed by individual proteins (probably twice a few lipid layers, although new calculations[22] suggest that the range could be longer). Finally, the interaction may not satisfy the usual pairwise additivity assumption. For example, at high protein density, the lipids perturbed by different proteins may begin to overlap, and the total amount of perturbed lipid then clearly will not be the sum of the lipid perturbed by each protein; see Figure 2. For more information on the theories, the reader is referred to Reference 16; the growing experimental evidence supporting the notion of lipid-mediated interactions is reviewed in subsequent sections.

D. Effective Interactions

In the previous section, we noted that interactions between proteins and lipids can influence protein distribution and that this phenomenon can be explained by postulating the existence of a lipid-mediated protein-protein force. In fact, it is generally true that the distribution of a solute in a solution will be influenced by the properties of the solvent, as well as by the direct forces that act between solute particles. Unfortunately, explicitly treating such solvent-mediated effects is a formidable theoretical problem, and thus it is standard to adopt the so-called "McMillan-Mayer description" of fluids, in which only the solute is treated explicitly.[19,23] If this description is adopted, all of the formulae that relate interactions to organization and mobility in a one-component fluid can be applied to a multicomponent (solute + solvent) fluid, if the solute-solute interaction is first averaged over solvent effects. (Such averaging can lead to deviations from pairwise additivity.) In the sections that follow, we will adopt the McMillan-Mayer formalism and will use the terminology "effective interaction" to remind the reader that the force appearing in all formulae has been averaged

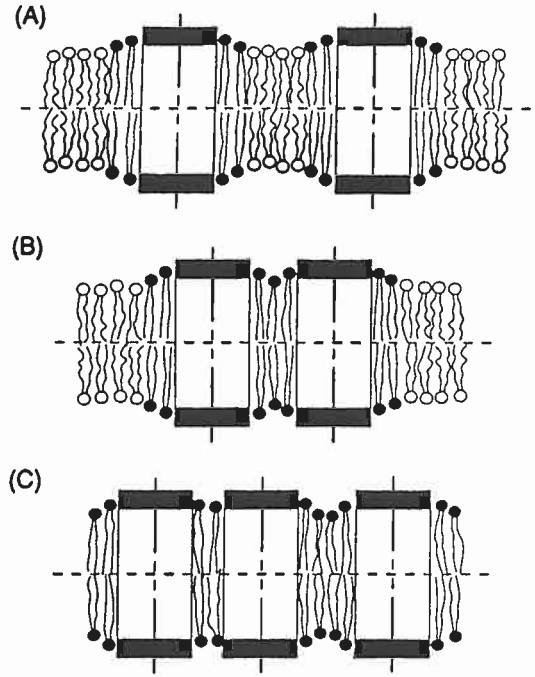

FIGURE 2. Origins of lipid-mediated protein-protein interactions. Proteins are again viewed normal to the plane of the membrane. (A) Proteins are surrounded by annuli of "perturbed" lipids (black head groups). The perturbations arise as lipids match headgroups to hydrophilic protein domains (dark stippling) and hydrocarbon chains to hydrophobic protein domains (light stippling). (B) If the perturbation of lipid is energetically unfavorable, then the total amount of unfavorably perturbed lipid can be minimized by protein aggregation, which allows proteins to share perturbed lipid. (For the particular longitudinal section depicted here, there are two less perturbed lipids when the two proteins aggregate.) This aggregation is effectively driven by an attractive lipid-mediated protein-protein interaction. If the perturbation of lipid is sufficiently different for unlike proteins, close association of protein can be energetically less favorable than wide separation, and proteins will spread apart (not shown). This dispersal is effectively driven by a repulsive lipid-mediated protein-protein interaction. (C) At very high protein concentrations, all of the lipid in the membrane may be perturbed. Protein movement then can neither increase nor decrease the total amount of perturbed lipid, and the lipid-mediated interaction is said to be saturated.

over solvent effects; the force may thus contain both direct and indirect (solvent-mediated) components.

III. SHORT RANGE PROTEIN ORGANIZATION

Over distance scales that extend out to several times the average interprotein spacing, protein molecules exhibit a short range organization that is profoundly

affected by protein-protein interactions. Here a theoretical formalism is developed that relates short range protein organization to the forces that act between proteins. The predictions of this formalism are explored through numerical simulation. Applications to biological membranes are made using information on short range protein organization that can be obtained from freeze-fracture electron micrographs.

A. Theoretical Description

Consider a patch of membrane containing a protein species, assorted lipid species, water, and other components. Assume that this patch can be modeled as an equilibrated fluid, about which one has information only on the center-of-mass coordinates of the protein species. It is now shown that statistical summaries of the center-of-mass positions of the proteins can be made in terms of probability densities known as distribution functions. These, in turn, can be related to protein-protein forces through the statistical mechanical theory of fluids,[18,19,23,24] which is a fairly natural theory to apply to a fluid-mosaic membrane.[25]

1. Distribution Function Formalism

Distribution functions describe the probability of finding certain equilibrium arrangements of molecules in a fluid. Specifically, the probability density $\rho^{(n)}(\vec{r}_1,\ldots,\vec{r}_n)$ is a measure of the probability of finding a particle at $\vec{r}_1$, a particle at $\vec{r}_2$,..., and a particle at $\vec{r}_n$ in a fluid of N indistinguishable particles at equilibrium. We argued qualitatively in the Introduction that a distribution such as $\rho^{(n)}(\vec{r}_1,\ldots,\vec{r}_n)$ should be related to the interactions between the particles. A rigorous version of that argument yields the following relationship:

$$\rho^{(n)}(\vec{r}_1,\ldots,\vec{r}_n)=\frac{N!}{(N-n)!}\int\ldots\int\frac{\exp\left[-U_N(\vec{r}_1,\ldots,\vec{r}_N)/k_BT\right]d\vec{r}_{n+1}\ldots d\vec{r}_N}{Z_N} \quad (6)$$

where Z_N is the configuration integral of the canonical partition function. The magnitude of the interaction dependence is thus scaled by the thermal energy, k_BT, in the system. Note that only the positions of the n (protein) particles of interest are specified; the positions of the remaining N–n particles are eliminated by integration. In addition, Equation 6 has already been integrated over solvent degrees of freedom, making U_N an effective interaction energy in the McMillan-Mayer sense.

Despite these simplifications, Equation 6 remains a complicated relationship that does not immediately impart an intuitive feeling for how interactions affect distribution. However, some physical intuition can be developed by analyzing Equation 6 in more detail. Consider first what distribution functions look like in the *absence* of interactions. In this case $U_N = 0$, and Equation 6 reduces to

$$\rho^{(n)}\left(\vec{r}_1,\ldots,\vec{r}_n\right) = N(N-1)\ldots(N-n+1)\left[V^{N-n}/V^N\right] \approx N^n/V^n = \rho^n \quad (7)$$

where ρ is the average number density. Thus, for an ideal (noninteracting) fluid, $\rho^{(n)}\left(\vec{r}_1,\ldots,\vec{r}_n\right)$ is independent of position and equal to ρ^n when $N >> n$ (which is almost always the case). In contrast, consider next what distribution functions look like in the *presence* of interactions. In this case, $\rho^{(n)}\left(\vec{r}_1,\ldots,\vec{r}_n\right)$ is dependent on position, and in the large N limit it is possible to specify this position dependence by defining a correlation function, $g^{(n)}\left(\vec{r}_1,\ldots,\vec{r}_n\right)$ by

$$\rho^{(n)}\left(\vec{r}_1,\ldots,\vec{r}_n\right) \equiv \rho^n g^{(n)}\left(\vec{r}_1,\ldots,\vec{r}_n\right) \quad (8)$$

Thus, for nonideal (interacting) fluids, the quantity $g^{(n)}\left(\vec{r}_1,\ldots,\vec{r}_n\right)$ gives a simple measure of the deviation of $\rho^{(n)}\left(\vec{r}_1,\ldots,\vec{r}_n\right)$ from ρ^n. In fact, Equation 8 shows that values of $g^{(n)}\left(\vec{r}_1,\ldots,\vec{r}_n\right)$ that differ from unity are indicative of nonideal correlations in particle positions.

2. *Examples of Distribution Functions*

The $n = 1$ distribution function, $g^{(1)}\left(\vec{r}_1\right)$, describes the spatial variation in single particle density. In a crystal, a particle is most typically located at a lattice site, and $g^{(1)}\left(\vec{r}_1\right)$ will have pronounced maxima at these locations. However, in a homogeneous fluid (ideal or nonideal), a particle is equally likely to be found at any point, and $g^{(1)}\left(\vec{r}_1\right) = 1$ for all $\vec{r}_1$.

The $n = 2$ (pair) distribution function, $g^{(2)}\left(\vec{r}_1,\vec{r}_2\right)$, describes positional correlations between pairs of particles and is consequently more complicated than $g^{(1)}\left(\vec{r}_1\right)$. In a crystal, $g^{(2)}\left(\vec{r}_1,\vec{r}_2\right)$ will have pronounced maxima whenever $\vec{r}_1$ *and* $\vec{r}_2$ correspond to the locations of lattice sites. In contrast, in a homogeneous fluid, $g^{(2)}\left(\vec{r}_1,\vec{r}_2\right)$ is a complicated function of $\vec{r}_1,\vec{r}_2$, particle density, temperature, and the interparticle force, as will be seen in subsequent sections. The pair distribution function can be simplified by rewriting it in a conditional form, $g(\vec{r}\,)$, where $\rho g(\vec{r}\,)d\vec{r}$ gives the number of molecules in an area $d\vec{r}$ about $\vec{r}$ *given* that there is a molecule at the origin. In a homogeneous fluid, the pair correlation function is termed the radial distribution function, written simply as $g(r)$, where $r = |\vec{r}_2 - \vec{r}_1|$; see Figure 3. (The vector $\vec{r}$ here is replaced by its magnitude, r, because in a homogeneous fluid the distribution does not depend on direction.) The radial distribution function has played a pivotal role in the theory of three-dimensional fluids for two reasons. First, it can be determined experimentally from scattering data. Second, thermodynamic functions and transport properties can be written in terms of $g(r)$ and $u(r)$ if the total interaction energy is pairwise additive.

High-order distribution functions ($n \geq 3$) relate positional correlations among still higher numbers of particles. In a homogeneous fluid, the conditional triplet correlation function can be written $g^{(3)}(r,s,q)$, where $s = |\vec{r}_3 - \vec{r}_1|$ and $q = |\vec{r}_3 - \vec{r}_2|$;

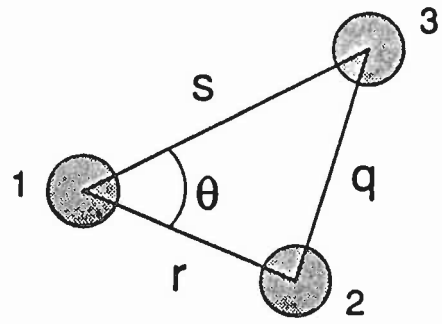

FIGURE 3. Polar coordinate system used for two and three-particle distribution functions. The positions of particles 1, 2, and 3 are specified by the vectors $\vec{r}_1$, $\vec{r}_2$, and $\vec{r}_3$, respectively, relative to an arbitrary origin (not depicted). The relative positions of 1, 2, and 3 are specified by the vectors $\vec{r} = \vec{r}_2 - \vec{r}_1$, $\vec{s} = \vec{r}_3 - \vec{r}_1$ and $\vec{q} = \vec{r}_3 - \vec{r}_2$, with magnitudes r, s, and q.

see Figure 3. For three-dimensional fluids, such high-order distribution functions cannot normally be measured, and it is usually assumed that the "superposition approximation" holds, i.e., that

$$g^{(3)}(r,s,q) = g(r)g(s)g(q) \quad (9)$$

In contrast, for two-dimensional membrane systems, $g^{(3)}(r,s,q)$ can be measured, and this facilitates a more accurate determination of the protein-protein force[26–29] as well as a more complete description of membrane protein diffusion.[30]

3. *Multicomponent Distribution Functions*

All of the distribution functions mentioned above can be generalized to describe systems containing two or more species of protein. The associated equations are not presented; instead it is simply noted that the generalization requires distinguishing each molecular species present. For example, if there are two species of protein, A and B, then three radial distribution functions must be introduced: $g(r_{AA})$, $g(r_{BB})$, and $g(r_{AB})$. These quantities determine the probability of finding a particle of type i at a distance r_{ij} from a given particle of type j. (By symmetry, $g(r_{AB}) = (r_{BA})$.)

B. Computation of Distribution Functions

We now turn attention to describing methods used to calculate distribution functions from experimental data. For simple three-dimensional systems, the radial distribution function can be determined experimentally from scattering data by computing the Fourier transform of the structure factor.[18,19,24]

Alternatively, for some two-dimensional systems in which molecular positions are known, distribution functions of arbitrary order can be determined directly using their probabilistic definitions. This latter procedure is described here for the radial distribution function; the generalization to high-order distribution functions is straightforward.[31]

As noted above, the quantity $\rho g(r)A$ is the number of particles in an annulus of area A bounded by $r-dr/2$ and $r+dr/2$ about a given central particle. Therefore, if molecular positions are known, $g(r)$ may be calculated using the following prescription. Approximate the infinitesimal increment dr by a small bin of finite width Δr, which ideally is only a few percent of the average interparticle spacing in the system. Focus attention on a particular particle and value of $r_i = n_i \Delta r$ (where $n_i = 1,\ldots,n_{max}$), and count the number of particles in the annulus bounded by $r_i - \Delta r/2$ and $r_i + \Delta r/2$ about the chosen particle. Divide this number by $\rho\pi[(r_i + \Delta r/2)^2 - (r_i - \Delta r/2)^2]$, which is the expected number of particles in the annulus. For each value of n_i, repeat this procedure for each particle in the system, and average the results. Equation 10 summarizes the algorithm.

$$g(r) = \langle g(r_i = n_i \Delta r) \rangle = \Sigma \frac{\text{number of particles in annulus bounded by } r_i - \Delta r/2 \text{ and } r_i + \Delta r/2}{\rho\pi\left[(r_i + \Delta r/2)^2 - (r_i - \Delta r/2)^2\right]} \quad (10)$$

A schematic view and a few caveats are presented in Figure 4.

To determine how physical properties of the system, such as particle density and interaction potential, affect distribution functions, it is necessary to have some method of generating molecular coordinates. This can be accomplished numerically through Monte Carlo simulations and experimentally through freeze-fracture electron microscopy. The numerical approach is discussed first.

C. Monte Carlo Simulations

The theory presented previously rigorously connects the short range organization of proteins, as embodied in distribution functions, to the effective forces that act between proteins, given that a few assumptions about the nature of the membrane hold. Unfortunately, the theories are quite complicated and can be solved analytically for quantities such as the radial distribution function or the effective interprotein force only at low protein density (ρ small). However, if numerical methods are exploited, one can obtain a wealth of information about distributions or effective forces for fluids of arbitrary density. We now describe a numerical method, Monte Carlo simulation, that is well suited for simulating the properties of fluids and discuss what numerical simulations have revealed about the short range organization of interacting particles in two-dimensional fluids such as membranes.

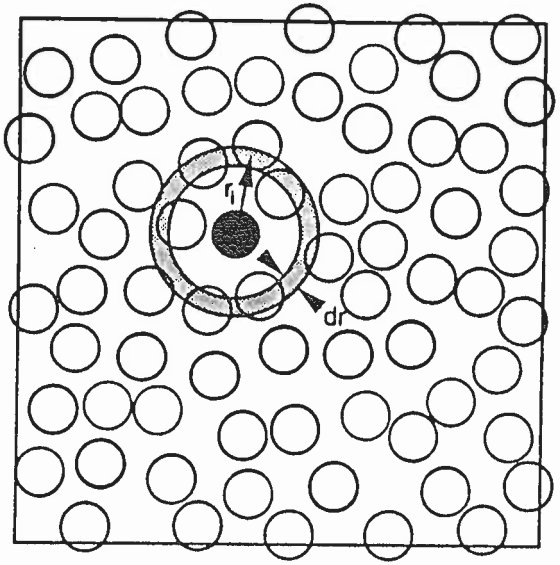

FIGURE 4. Computation of radial distribution functions. Distribution functions can be computed from particle positions by implementing the prescription given in Equation 10 as follows. Here the unit of length is taken to be the particle diameter, d. Consider first a single annulus (indicated by stippling) of radius $r_i = 1.55d$ and width $dr = 0.39d$ about a single protein (indicated in black). (Note that the width of the annulus has been much exaggerated for clarity.) The average density of the configuration, $\rho = 0.58/d^2$, is the number of particles in the box, $N = 70$, over the area of the box, $A = 120d^2$. Since the annulus contains the centers of three proteins, the density of proteins in the annulus, $\rho = 0.79/d^2$, is simply 3 over the area of the annulus, $3.80d^2$. Hence, the ratio of the observed to the expected number of proteins in the given annulus is $[0.79/d^2]/[0.58/d^2] = 1.36$. If this computation is repeated for all particles in the configuration and the results averaged, one will obtain $g(1.55d)$. Clearly, edges require special consideration and can be handled in a variety of ways.[31,92]

1. *Overview of Algorithm*

Monte Carlo is an efficient method of determining ensemble-averaged, *equilibrium* properties of a system, such as distribution functions. This is accomplished using an ingenious strategy known as "importance sampling." Probability theory states that averaged quantities can be obtained by summing (or integrating) the variable of interest against an appropriate probability distribution, which for the canonical ensemble is the Boltzmann distribution, $exp[-U_N/k_BT]$. Thus, to determine an ensemble-averaged distribution function, Equation 10 must be evaluated for many configurations (corresponding to a desired density and interaction potential) and the results then weighted by the Boltzmann factor and averaged. If configurations are chosen randomly, most will be far from equilibrium and contribute only slightly to the average. However, if configurations are chosen with a probability given by their Boltzmann

factor (i.e., by importance sampling), almost all will be near equilibrium and all will contribute equally to the average. The difference in efficiency between random sampling and importance sampling can be astronomical: easily a googol.

Monte Carlo simulations are inevitably performed on a computer, although different algorithms can be employed to implement the importance sampling. The classic is the Metropolis Monte Carlo algorithm.[32] To simulate protein positions using this approach, proteins are initially assigned arbitrary positions in some (two-dimensional) space. The number of proteins and the area of the space determine the density. Of course, this arbitrary initial configuration will not necessarily be near equilibrium for the interaction potential and density of interest, and so protein positions must be changed until equilibrium is approached. This is accomplished by randomly trying to move particles in the system and then comparing the energy of the new "trial" configuration to the energy of the old configuration. If the changes in position lower the energy of the system, they are automatically accepted. If the changes raise the energy, a "dice-roll" rule employing the Boltzmann factor is used to determine acceptance or rejection of the new configuration. If this procedure is repeated many times, it can be shown that the configurations eventually approach equilibrium corresponding to the chosen interaction potential and density.[32] Moreover, once this has occurred, all subsequent configurations generated by the technique will also be near equilibrium. Thus, properties computed from many such configurations will be canonically averaged, according to the Boltzmann distribution.

Monte Carlo is a powerful technique that has literally revolutionized the study of fluids. However, the technique can be subtle and a word of caution is in order. The importance-sampling algorithm makes fundamental assumptions about the physics underlying equilibrium. The Metropolis algorithm describes the canonical ensemble: closed systems with constant area and temperature. Other algorithms can be constructed to describe other ensembles. The chosen algorithm and ensemble must describe the system under study; otherwise, the results can be invalid, as shown in Reference 33. The fundamentals of Monte Carlo are reviewed in References 19 and 24, while applications to biological membranes are reviewed in Reference 34.

2. *Results*

Monte Carlo techniques have been used to simulate the effects that protein density and interparticle interactions have on the equilibrium distribution of membrane proteins; here we summarize the pertinent simulation results and explore their implications. In the Appendix, we briefly discuss relevant results obtained using related simulation techniques.

Effective interactions were studied that model the effects of both repulsive and attractive interactions on protein organization. The excluded-volume potential (Equation 3) was taken as a model of "hard" repulsions. An inverse-power-law potential was taken as a model of "soft" repulsions and long range attractions:[27,29,35]

$$u(r) = (27/4)k_BT\left[(\sigma/r)^6 - (\sigma/r)^4\right] \tag{11}$$

Here σ is where the potential crosses zero, and $(^3/_2)^{1/2}\sigma$ is where the potential attains its minimum value of k_BT. The effects of attractions on organization were determined by comparing simulation results based on Equation 11 with simulation results based on a potential with identical repulsions but no attractions derived from a Weeks-Chandler-Andersen decomposition[36] of Equation 11. Both long range potentials are shown in Figure 5. Simulation results are available in terms of particle configurations, which may be examined visually, and radial distribution functions, which provide a statistical summary of the coordinate information.

The particle configurations provide a qualitative picture of protein organization in membranes; see Figure 6. For example, the configurations clearly suggest that interactions lead to short range ordering within the membrane, since particles do not approach one another very closely. In addition, the configurations provide evidence that interactions lead to some long range ordering. For example, protein distribution in the presence of attractions appears to manifest a tendency toward "patchiness."

To analyze organization more quantitatively, radial distribution functions can be computed from the particle configurations using the prescription given in Equation 10. Typically, results from many independent configurations are averaged to get good statistics. The distribution functions are typical of those found for interacting fluid systems; see Figure 7. At small separations, the probability of finding a second particle is zero, since the particles cannot approach one another very closely due to the strong short range repulsions. Thus,

$$\lim_{r\to 0} g(r) = 0 \tag{12}$$

At large separations, the probability of finding a second particle is random, since the interaction is of finite range and correlations in particle position do not extend indefinitely over space. Thus,

$$\lim_{r\to \infty} g(r) = 1 \tag{13}$$

At intermediate separations, there are regions of enhanced and diminished probability of finding second particles. These "coordination shells" are manifest as "peaks" and "valleys" where the values of $g(r)$ are greater than and less than one, respectively.

The Monte Carlo data show how differences in density and interaction potential affect $g(r)$; see Figures 6 and 7. At low protein density, particle configurations and radial distribution functions derived from the attractive and repulsive potentials shown in Figure 5 differ considerably, whereas at high

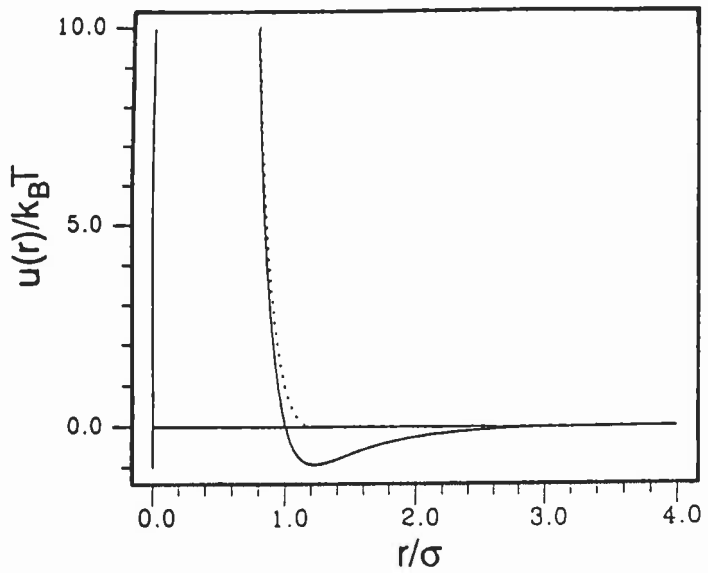

FIGURE 5. Analytical pair potentials employed in Monte Carlo simulations. Purely repulsive (dotted) and attractive-plus-repulsive (solid) interactions were defined by Equation 11 and a Weeks-Chandler-Andersen decomposition.[27] These interactions were studied because they qualitatively resemble the relatively soft repulsions and weak, long range attractions predicted to act between membrane proteins. Note that when the two potentials are differentiated, the repulsive components of the resulting forces are identical. (From Abney, J. R. and Owicki, J. C., *Chem. Phys. Lett.*, 164, 73, 1989. With permission.)

density they appear very similar. Such a density and interaction dependence arises because, at low densities, attractive interactions induce partial aggregation of the solute. This leads to greater short range organization in the presence of attractions and a better defined structure in the radial distribution function. In contrast, at high density, particles are so close together that further aggregation cannot occur. Repulsions then dominate organization,[36,37] and, consequently, $g(r)$ has a similar, highly structured appearance for both fluids. Modern perturbation theories of fluids[18,19,36] are based on the fact that repulsions dominate fluid structure at high density.

D. Freeze-Fracture Electron Microscopy

In the previous section, it was shown that numerical methods can be used to obtain information on the distribution of interacting membrane proteins. Such information can also be obtained experimentally using freeze-fracture electron microscopy.[38]

1. Overview of Technique

Freeze-fracture electron microscopy provides a method of visualizing the

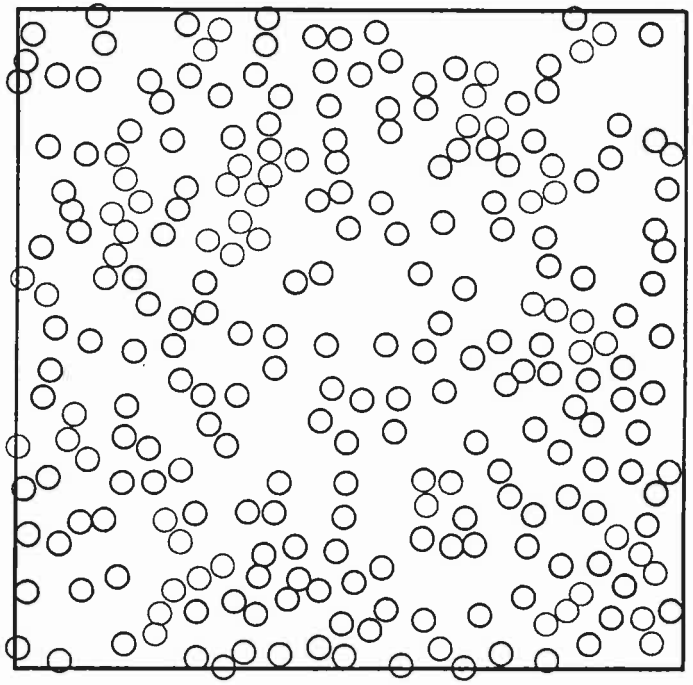

FIGURE 6. Particle configurations for purely repulsive and attractive-plus-repulsive interactions at relatively low and high concentrations. Configurations containing 256 particles were generated by Monte Carlo simulation for the two potentials shown in Figure 5 at two different reduced densities, $\rho^* \equiv \rho\sigma^2$. The configurations correspond to (A) purely repulsive potential, $\rho^* = 0.3$; (B) attractive-plus-repulsive potential, $\rho^* = 0.3$; (C) purely repulsive potential, $\rho^* = 0.8$; and (D) attractive-plus-repulsive potential, $\rho^* = 0.8$. In all cases, periodic boundary conditions were invoked. The dominance of attractions at low densities is reflected in the marked tendency toward "patchiness" in Panel B relative to Panel A, while the dominance of repulsions at high densities is reflected in the similarity of Panels C and D.

positions of individual proteins in membranes. In the freeze-fracture technique, the sample of interest (a small piece of tissue, a drop of suspended vesicles, etc.) is rapidly frozen. If the freezing is rapid enough,[27] the process preserves a snapshot of the sample as it existed at the time of freezing, and the relative positions of membrane proteins are thus preserved. If the frozen sample is then fractured, the cleavage plane tends to run preferentially between the two leaflets of the bilayer, and protein positions are manifest as pits and bumps on an otherwise smooth surface. A replica of this surface can be prepared by shadowing with a heavy metal to give contrast and then stabilizing the shadow with a carbon film. This replica can be viewed under the electron microscope, and the positions of individual proteins observed. Distribution functions can be determined directly from the electron micrographs by digitizing protein positions and then following the prescription given in Equation 10. See Figure 8.

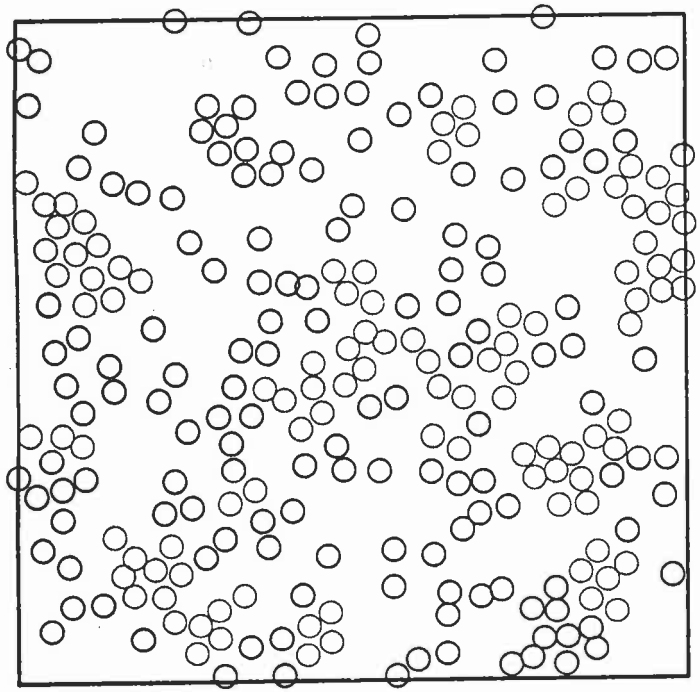

FIGURE 6B.

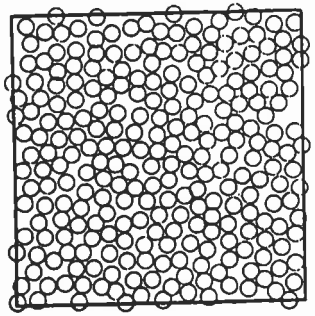

FIGURE 6C.

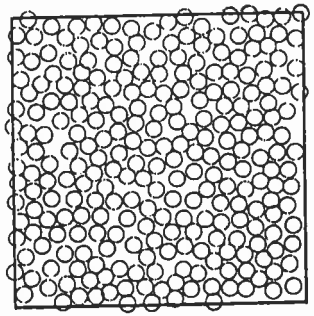

FIGURE 6D.

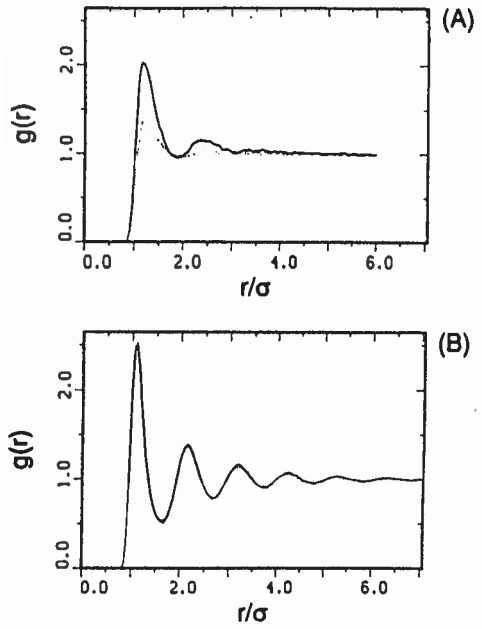

FIGURE 7. Radial distribution functions for purely repulsive and attractive-plus-repulsive interactions at relatively low and high concentrations. Distribution functions were computed for the two potentials shown in Figure 5 using the configurations shown in Figure 6 and the prescription outlined in Figure 4. Results were averaged over bins of width Dr = 0.05r every 10 cycles for a total of 2000 to 5000 cycles (i.e., results were averaged over 200 to 500 configurations). A cycle corresponds to one sequentially attempted perturbation of every particle in the system. The radial distribution function gives a measure of the order in the fluid as a function of radial distance, r. Order is lowest for $r^* = 0.0$. As the density of the system is raised, order increases and coordination shells develop, corresponding to regions of enhanced ($g > 1$) and diminished ($g < 1$) occupancy. Concomitantly, the average center-to-center distance, determined by the location and area of the first peak in $g(r)$, decreases. (A) At $r^* = 0.3$, particles are significantly closer in fluid A (solid line) than in fluid R (dotted line), brought together by attractive interactions. (B) At $r^* = 0.8$, the identical repulsions dominate the structure of both fluids, and the two distribution functions are virtually superimposable. For these potentials, the continuous initial rise in $g(r)$ has its origin in the soft potential used in the simulations. In contrast, a discontinuous initial rise is observed in simulations of radially symmetric excluded-volume potentials. (From Abney, J. R. and Owicki, J. C., *Chem. Phys. Lett.*, 164, 73, 1989. With permission.)

Like Monte Carlo, freeze fracture is a powerful technique that cannot be applied without caution. High resolution studies, such as those described here, require very rapid freezing to minimize protein rearrangements. In addition, replicas should be free of plastic deformation and should be of sufficient quality to resolve individual proteins. Finally, some of the studies discussed here require that the membrane contain only a single type of protein free of cytoskeletal constraints.

2. Results

Freeze-fracture (and closely related freeze-etch) techniques have been extensively used to study membrane architecture, and they are a significant source of information on membrane heterogeneity. Although the focus is typically on long range organization, freeze-fracture pictures can also be used to study short range organization. Here we describe those studies ultimately aimed at relating short range protein organization to protein-protein interactions through the use of distribution functions. In the Appendix, we briefly discuss relevant results obtained from purely statistical methods.

Distribution functions have been used to characterize the short range organization of proteins in a variety of systems. In some of these systems, the identity of the proteins under study was well defined: nuclear pores,[39] gap junction connexons,[26,28,40] various virus particles,[40,41] surface immunoglobulin,[42] rhodopsin,[43] and BR.[43] In other systems, the proteins under study were less well characterized and only the membrane was identified: mouse fibroblasts,[40] human and pig erythrocytes,[44-46] barley cells,[45] and *A. laidlawii*.[47] Especially clean radial distribution data have been obtained for gap junctions, because in this system there is only one protein species and the positions of proteins are not influenced by cytoskeletal constraints (see Figure 9).

For essentially all of the systems studied, $g(r)$ was found to have a fluid-like form, rising from zero at small r, displaying one or more oscillations at intermediate r, and finally decaying to one at large r. This functional form confirms the fluid-like character of the membrane and demonstrates that the protein molecules interact, since in the absence of interaction $g(r) = 1$ for all values of r. However, the precise functional form of the interaction cannot immediately be deduced simply by looking at $g(r)$. This is because the radial distribution function depends on many variables, including density, interaction potential, molecular shape, and the distribution of particle sizes. In the next section, it is demonstrated that one can extract the precise form of the effective interaction from a knowledge of distribution functions.

IV. MEASUREMENT OF PROTEIN-PROTEIN INTERACTIONS

In this section, we move away from the realm of postulated forces and describe experimental attempts to measure the real forces that act between proteins in membranes. Such measurements have a twofold purpose. First, they might provide verification for theories of protein-protein interactions. For example, is there evidence for a lipid-mediated protein-protein interaction as suggested by theory? Second, they facilitate determination of thermodynamic and kinetic properties of the membrane, even in the absence of a detailed understanding of the origins of the measured forces, as will be seen later.

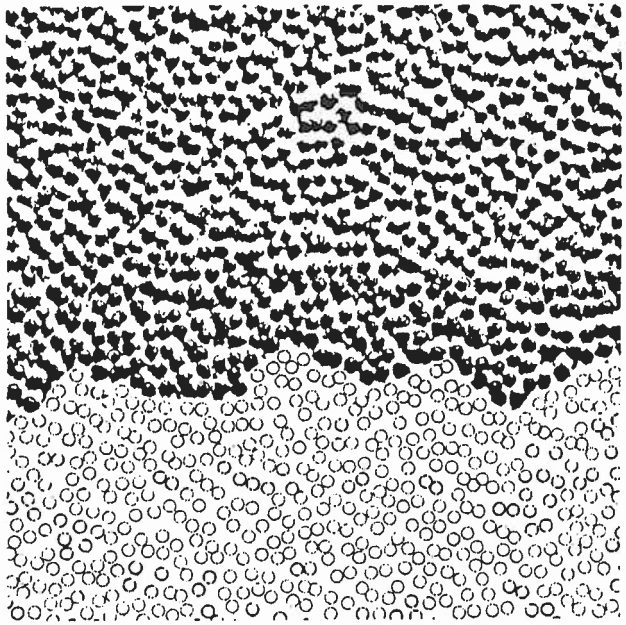

FIGURE 8. High magnification enlargement of an electron micrograph of a mouse liver ga junction segued into a digitized computer representation. The region shown was in the interior of th junction; the junction boundary is not visible. In the micrograph (upper region) proteins are visib as "bumps" against the comparatively smooth membrane interior. The junction contains only a sing type of protein, aggregated into a plaque at a density of 9,330 proteins/μm². The computer repr sentation (lower region) shows particle coordinates obtained by manually digitizing the micrograp using a computer digitization tablet. Proteins are drawn to their 7 nm crystallographic diameter, an protein positions are probably accurate to within 0.5 to 1.0 nm. The computer representation wa compared with the original micrograph to check for misentered or missing particles. (After Abne J. R., Braun, J., and Owicki, J. C., *Biophys. J.*, 52, 441, 1987. With permission.)

A. The Inverse Problem

The exact analytical expressions relating distribution functions and forces ar very complicated. Therefore, it is quite common to use numerical, rather tha analytical, methods to study interacting particles in fluids, as discussed previ ously. It is also quite common to make certain assumptions that simplify th analytical expressions (e.g., that pairwise additivity holds) and then to proceed with an analytical analysis of interacting particles in fluids. The simplifie analytical (integral) equations can be used to calculate distribution function from postulated forces and could therefore have been discussed in the previou section. However, the integral equation formalism was omitted previousl because the distribution functions it yields are approximate, whereas th

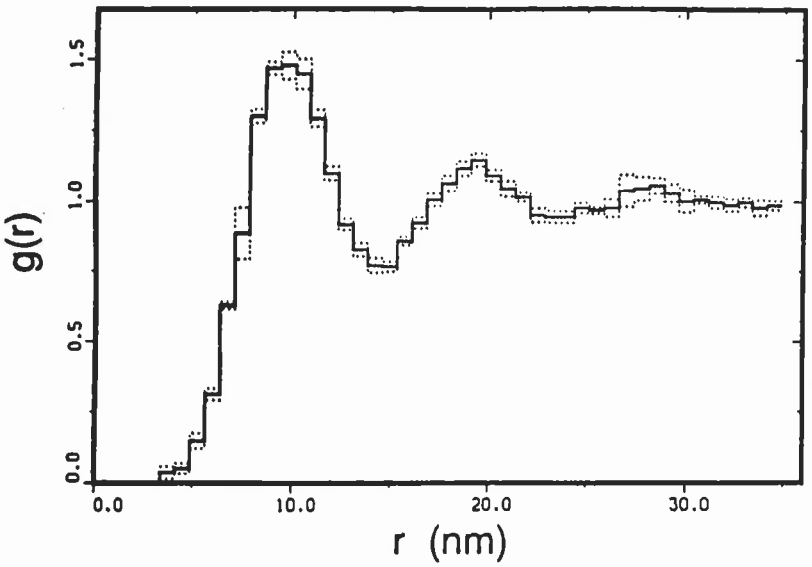

FIGURE 9. Radial distribution function for proteins within a mouse liver gap junction. The distribution function was computed using the prescription given in Equation 10 and bins of width Δr = 0.75 nm. The average center-to-center spacing of the proteins is approximately 10.6 nm, and up to three partially ordered coordination shells are visible. The distribution function is very reminiscent of that found for interacting particles in simple fluids (see Figure 7). The dotted error envelope gives a measure of the uncertainty in the distribution function and represents the standard deviation obtained by separate analysis of two regions of the same junction, each of which contained about 2000 particles. The small error bars suggest that there are only minimal differences between different regions of the same junction. Larger differences are seen when distribution functions are computed from different junctions.[28] (From Abney, J. R., Braun, J., and Owicki, J. C., *Biophys. J.*, 52, 441, 1987. With permission.)

distribution functions calculated using modern simulation methods are essentially exact. Here, we will focus on how integral equations can be used to deduce the form of the effective force from a measured distribution. This is the classic "inverse problem," which is not easily soluble using exclusively numerical methods.

There are many integral equations, and each involves a different set of assumptions. We focus here on the Percus-Yevick (PY) and Born-Green-Yvon (BGY) integral equations because they have been extensively exploited in studies of protein-protein forces in membranes. We present the equations and discuss those underlying approximations and assumptions that are pertinent to the issue of extracting protein-protein forces from protein distributions obtained from freeze-fracture electron micrographs; detailed derivations and more complete discussions of these equations can be found in most statistical-mechanics textbooks.[18,19,23]

1. The Percus-Yevick (PY) Equation

The PY equation is a relationship between the effective pair potential and the two-particle distribution function:

$$g(r)\exp\left[\frac{u(r)}{k_BT}\right] = 1 + \rho\int_0^{\infty} g(s)\left\{1-\exp\left[\frac{u(s)}{k_BT}\right]\right\}[g(q)-1]2\pi s\,ds \qquad (14)$$

The PY equation is based on pairwise additivity and the so-called PY approximation, which is meant to model approximately the effects of high-order correlations in the positions of molecules. The PY approximation and thus the PY equation are valid at low densities, where the range of the protein-protein force is smaller than the average interparticle separation. If the two-particle distribution function is known, the PY equation can be solved directly for the pair potential.

2. The Born-Green-Yvon (BGY) Equation

The Born-Green-Yvon equation is a relationship between the effective pair force and the two- and three-particle distribution functions:

$$k_BT\frac{d[\ln g(r)]}{dr} = f(r) + \rho\int_0^{\infty} f(s)\int_0^{2\pi}\frac{g^{(3)}(r,s,\theta)}{g(r)}s\cos\theta\,d\theta\,ds \qquad (15)$$

(Note that the BGY equation is written here in a polar coordinate system; see Figure 3.) Like the PY equation, the BGY equation is based on pairwise additivity. However, no additional approximations are involved, and the BGY equation is exact if the potential is pairwise additive. (The BGY equation does become approximate if the three-particle distribution function is not known and the superposition approximation, Equation 9, is invoked.) The left-hand side of the BGY equation represents the statistical mean force on a particle.[18,19,23] The BGY equation shows that the mean force arises from two sources: the direct force exerted by the particle at r, $f(r)$, and the components along r of the forces exerted by particles at all other positions in the plane, the integral. If the two- and three-particle distribution functions are known, the BGY equation can be solved for the pair force. The pair force can then be integrated to yield the pair potential.

3. Comparison of the PY and BGY Equations

Both the PY and BGY equations can be used to extract important information on interparticle interactions. The primary advantage of the PY equation is that it involves only the two-particle distribution function, and thus when $g(r)$ alone is known, as is the case for three-dimensional fluids, the PY equation is typically invoked. However, the PY equation is not exact, and the significance of the

potential derived from the PY equation is obscured by this fact. The primary advantage of the BGY equation is that it allows the determination of effective pair potentials without recourse to approximation (if pairwise additivity holds). Thus, when both the two- and three-particle distribution functions are known, the BGY equation is the equation of choice.

The accuracy to which the PY and BGY equations reproduce the interaction generating a given distribution has been carefully tested.[27,29] In the test studies, Monte Carlo simulations were used to generate particle configurations and distribution functions for the purely repulsive and attractive-plus-repulsive potentials shown in Figure 5. The distribution functions were then inserted into each equation and solutions for the potential that generated the distributions obtained. Accuracy was determined by assessing how well each equation reproduced the starting potentials that were used to generate the distributions. It was found that the PY equation did not yield an accurate potential for protein concentrations typical of biological membranes; in contrast, the BGY equation was accurate for particle concentrations ranging from infinite dilution to crystal packing.

At low particle concentrations, the PY and BGY equations become identical, reducing to the "Boltzmann-like" relationship

$$g(r) = \exp\left[-u(r) / k_B T\right] \tag{16}$$

This relationship shows that the structure of the fluid is determined entirely by pair interactions at low particle densities, which is reasonable since at low densities high-order interactions will be negligible.

B. Application to Freeze-Fracture Electron Micrographs

Two different methods have been used to characterize the real effective forces exerted by membrane proteins. In the first (indirect) method, real protein distribution functions were computed from freeze-fracture data, and an attempt was then made to fit the data by postulating forms for the force and using an integral equation or Monte Carlo simulation to calculate theoretical $g(r)$s against which the experimental data were compared. The postulated force that yielded the best agreement between theory and experiment was then identified as the most likely interprotein force. In the second (direct) method, real distribution functions were again computed from freeze-fracture data. However, these distribution functions were then inserted into an integral equation and the equation solved directly for the real effective force that gave rise to the measured distributions. The first method has been more extensively exploited, but the second method yields more satisfying results.

For a variety of native membranes, a comparison has been made between theoretical and experimental $g(r)$s in an attempt to characterize interprotein

interactions. In the simplest of these studies, the distributions of intramembrano particles on pig erythrocytes,[46] surface immunoglobulin on mouse B lymph cytes,[42] and virus-related molecular assemblies on the surfaces of mou fibroblasts[40] were examined. Radial distribution functions were computed fro experimental data and compared with the distribution function for particles in noninteracting system ($g(r) = 1$ for all r). For all three systems, it was conclude that protein positions were influenced by nonidealities, but no attempt was mac to elucidate the precise nature of the interactions influencing distribution, e.g attractive vs. repulsive, short-range vs. long-range, etc.

In the remaining studies, a more serious attempt was made to identify th protein-protein force dictating distribution. These more sophisticated studi have focused on a relatively small number of membrane systems and a therefore discussed on a system-by-system basis.

1. *Human Erythrocyte Membranes*

Radial distribution functions have been most extensively used to characteriz protein organization in the erythrocyte membrane. As was the case with th systems mentioned previously, computation of $g(r)$ for erythrocyte protein immediately demonstrated that distribution was nonideal. In fact, the short rang organization of human erythrocyte proteins mirrors closely the theoretic organization of cylindrical proteins interacting through a repulsive force whos range slightly exceeds the proteins' excluded-volume diameter.[44] Howeve erythrocyte distribution functions, as well as those of a barley mutant, can als be fit to the theoretical distribution of elliptical particles interacting purel through an excluded-volume force.[45] It is thus clear that the form of the interac tion deduced from distribution functions is somewhat sensitive to particle shap a fact that illustrates that distribution functions are indeed complicated functior of many variables.

2. *Nuclear Membranes*

The radial distribution function of nuclear pores has been followed as function of cell type and stage in the cell cycle.[39] The data show that during th S phase of the human lymphocyte and HeLa cell cycles, the pore radia distribution function is structureless (i.e., is always unity), whereas during the G phase of the human lymphocyte cell cycle and the early G1 phase of the HeL cell cycle, the distribution function is structured. Thus, pore distribution appea to vary during the cell cycle. The interactions giving rise to these different por distributions were tentatively identified by inserting various repulsive force into the PY equation and calculating the associated $g(r)$s. The experimenta distribution functions were reasonably reproduced assuming a long rang repulsive interaction between S-phase pores and a short range excluded-volum repulsive interaction between G1 and G0 pores. Unfortunately, the origins an biological significance of these forces were not identified.

3. Acholeplasma laidlawii *Membranes*

Distribution function approaches have shown that lipid-protein interactions may be responsible for the aggregated state of proteins in *A. laidlawii* membranes.[47] This was demonstrated by deriving an explicit functional form for the lipid-protein interaction and using the PY equation to calculate the associated distribution function. It was possible to reproduce a number of different distribution functions derived from *A. laidlawii* membranes containing different protein densities simply by varying the strength of the lipid-protein interaction and its correlation length.

4. *Reconstituted Membranes*

One criticism that can be leveled against the work discussed above is that the systems under study were multicomponent, whereas the simulations and equations used to analyze the data rigorously model the properties of fluids containing only a single solute species. Reconstitution of a single membrane protein species into artificial bilayers can be used to overcome this problem. Reconstitution is also useful because it is well suited for precisely characterized manipulations of lipid composition and protein concentration, although it can induce unfavorable membrane curvature and lead to a loss of protein asymmetry.

Two proteins, BR and rhodopsin, have been studied by reconstitution into a variety of membranes.[43] The distribution of reconstituted BR was always found to be consistent with a pure hard-disk repulsive interaction between molecules, independent of the structure of the host lipid. In contrast, the distribution of rhodopsin suggested that the molecules were interacting through a longer range, possibly electrostatic repulsive interaction. However, in the thickest membrane (di 18:1 *trans*-PC), rhodopsin exhibited a partially aggregated distribution consistent with the existence of attractive lipid-mediated protein-protein interactions. Apparently when the membrane is thinner than the protein, the stretching of lipid required to match lipid and protein domains does not propagate significantly through the bilayer, and therefore no lipid-protein interaction results. However, when the membrane is thicker than the protein, lipid tilt (or some other conformational change) does propagate through the bilayer, and a lipid-mediated interaction results that significantly affects protein distribution.

5. *Gap Junctions*

Finally, we turn attention to the one study in which an integral equation has actually been inverted and a real effective force between membrane proteins directly measured.[26,28] The system analyzed, the mouse liver gap junction, was ideally suited to a fluid-theoretic study of forces because it contains only a single type of protein whose distribution is not determined by extramembraneous attachment. The interprotein force was obtained by inserting two- and three-particle distribution functions calculated from freeze-fracture data into the BGY equation. The force was found to be repulsive for all values of the interprotein

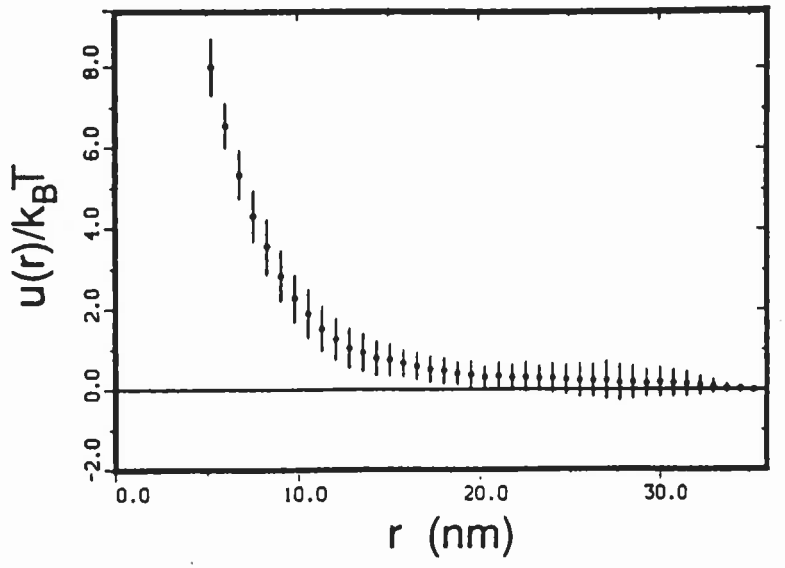

FIGURE 10. Effective pair potential for proteins within a mouse liver gap junction. The pair potential was determined by first computing the pair force using the BGY equation and then integrating the pair force to obtain the pair potential using Simpson's rule. The quantities inserted into the BGY equation were the radial distribution function (shown in Figure 9) and a three-particle distribution function (not shown). Analytical conditions were identical to those described in Figure 9. The vertical bars show the standard deviation associated with each value of the potential. The most significant feature of the potential is that it is everywhere repulsive, consistent with excluded-volume and electrostatic interactions between the identical junction proteins. (From Abney, J. R., Braun, J., and Owicki, J. C., *Biophys. J.*, 52, 441, 1987. With permission.)

spacing, r, and the associated potential (see Figure 10) was significant relative to thermal energies (k_BT) for $r \leq 12$ nm, i.e., over distances that exceed the average interparticle spacing in the system. The measured force is consistent with excluded-volume and electrostatic repulsion between gap junction proteins.

It might have been assumed *a priori* that protein molecules in the junction, which are highly aggregated, would interact through some sort of attractive force that induces aggregation. However, this is not the case; the force between junctional proteins was determined to be repulsive for all values of the interprotein spacing. Instead, the impetus for protein aggregation lies in interactions among junctional proteins and glycosylated proteins within the membrane; see Figure 11. To a first approximation, junctional proteins are immiscible with glycosylated membrane components, and protein aggregation into the junction represents a lateral phase separation that acts simply to separate immiscible species. At a more detailed level, the strength and range of the interactions fine-tune junction organization and help determine junction size and geometry.

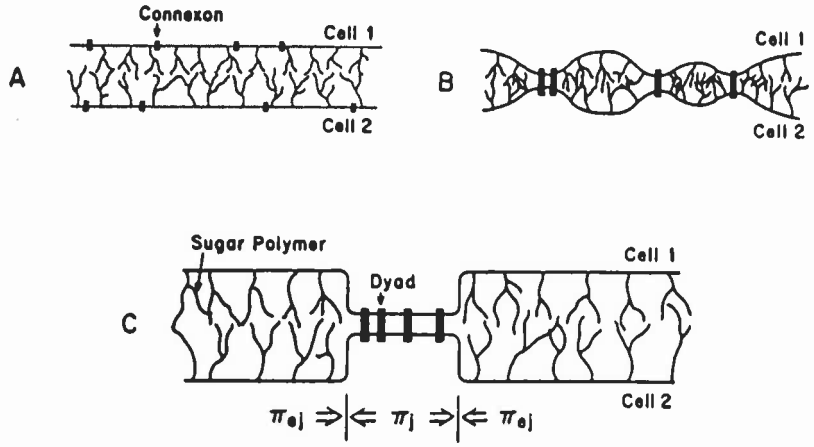

FIGURE 11. Pressure-balance model of the mouse liver gap junction. Gap junctions are dense aggregates of identical channel proteins that bridge the intercellular space between two closely apposed cells, thereby facilitating intercellular communication. The organization of the junction is not dictated by extramembranous constraints but rather reflects only interactions among membrane components. (A) Prior to junction formation, channel precursors (connexons) and the membrane anchors of the glycocalyx intermix. (B) Channel (dyad) formation occurs as connexons from neighboring membranes fuse through incompletely understood mechanisms. As a consequence of the fusion, adjacent regions of membrane are pulled into close proximity, leading to unfavorable interactions among elements of the glycocalyx. (C) These unfavorable interactions are minimized by a lateral phase separation that leads to the coalescence of the dyads to form the junction and the exclusion of the glycosylated species to form the extrajunctional glycocalyx. Junction size is maintained by a balance between a junctional pressure, Π_j, that arises from repulsions between dyads (Equation 17), and an extrajunctional pressure, Π_{ej}, that arises from interactions among sugar residues in the glycocalyx. (Interactions between sugar polymers in the glycocalyx, which can include elastic deformations, represent another type of protein-protein interaction not explicitly discussed in the text.) Bending near the edge of the plaque has been exaggerated to delineate more clearly the junctional and extrajunctional spaces. (From Abney, J. R., Braun, J., and Owicki, J. C., *Biophys. J.*, 52, 441, 1987. With permission.)

V. THERMODYNAMIC FUNCTIONS AND TRANSPORT PROPERTIES

To illustrate further the utility of distribution functions and effective forces, we now show that these quantities are related to thermodynamic and transport properties of simple nonideal fluids. Thus, freeze-fracture micrographs and an inverse-problem force analysis provide data that can be used to determine how thermodynamic and transport properties of the membrane are influenced by the membrane's nonideal, fluid-like character. Of course, fluid and nonfluid (e.g., cytoskeletal) effects must be considered in conjunction when analyzing the behavior of biological membranes, and the equations must be generalized if the membrane contains more than one protein species.

A. Thermodynamic Functions

If the particles in a simple fluid interact through pairwise-additive forces, all of the thermodynamic properties of the fluid can be expressed in terms of the radial distribution function and the effective protein-protein force. We focus here on computation of the osmotic pressure, because it has proven to be one of the more useful membrane properties;[28,35,48] the reader is referred to statistical-mechanics textbooks for other examples.[18,19,23,24]

Protein molecules behave like a solute in a lipid solvent and therefore contribute to the colligative properties of the membrane. The osmotic pressure, π, is a particularly familiar colligative property and is given by the pressure equation

$$\Pi = \rho k_B T + \left(\rho^2 / 4\right)\int_0^\infty rf(r)g(r)2\pi r dr \tag{17}$$

The first term in Equation 17 is ideal in origin (the van't Hoff equation), whereas the second term (which depends on the force and radial distribution function) is nonideal. In membrane systems, the nonideal term can make the dominant contribution to the total osmotic pressure,[28] and the osmotic pressure can probably deviate at least a fewfold from its ideal value.[28,35]

B. Transport Properties

As may be intuitively obvious, the mobility of membrane proteins is also affected by protein organization and interprotein interactions. In fact, theoretical expressions have already been derived that relate protein mobility to both distribution functions and forces. These expressions neglect the so-called hydrodynamic interaction, a dynamic protein-protein interaction mediated by protein-induced perturbation of solvent flow.

Two types of translational diffusion have been studied. The first, mutual diffusion, refers to the dissipation of gradients or fluctuations in protein concentration[49] and is the process monitored in postelectrophoresis relaxation experiments.[50] The mutual-diffusion coefficient, $D^m(\rho)$, is given by the expression[35,48,49]

$$\frac{D^m(\rho)}{D_0} = 1 + \frac{\rho}{2k_B T}\int_0^\infty rf(r)\left[g(r) + \frac{1}{2}\rho\frac{\partial g(r)}{\partial \rho}\right]2\pi r dr \tag{18}$$

where D_0 is the bare-diffusion coefficient, which describes protein diffusion in the absence of interaction (i.e., at infinite protein dilution).

The second, self diffusion, refers to the mean-square Brownian motion of individual proteins[49] and is the process monitored in fluorescence recovery after

photobleaching experiments.[51-53] The self-diffusion coefficient, $D^s(\rho)$, is given by the expression[14,30,49]

$$\frac{D^s(\rho)}{D_0} = 1 + \frac{\rho}{4k_BT}\int_0^\infty f(r)p(r)g(r)2\pi r dr \qquad (19)$$

where $p(r)$ is the solution of a complicated integrodifferential equation that depends on $f(r)$, $g(r)$, and $g^{(3)}(r,s,\theta)$.

Equations 18 and 19 have been used to demonstrate that interprotein interactions can have significant effects on the two diffusion coefficients. For example, at finite protein concentrations, interactions cause the two diffusion coefficients to differ. Moreover, in the absence of hydrodynamic interactions, each diffusion coefficient can differ a fewfold from its ideal value, D_0. See Reference 14 for a more detailed discussion.

VI. LONG RANGE PROTEIN ORGANIZATION

In the previous sections, it was demonstrated that protein-protein interactions can profoundly influence the short range organization of proteins within the membrane. In this section, we extend this basic concept and demonstrate that protein-protein interactions and membrane fluidity can also influence long range protein organization, i.e., organization over distance scales that range from several times the average interprotein spacing out to many microns.

Ideally, this section would be written in analogy with our discussion of short range organization and would begin with rigorous mathematical formulae that relate long range protein organization to interprotein interactions. The predictions of the formalism would then be compared with the appropriate experimental results. Unfortunately, there is no simple and unified (e.g., fluid theoretic) formalism that describes all of the complicated relationships between interactions and long range protein organization. Instead, these relationships must be explored on a case-by-case basis. Thus, here we examine the effects that protein-protein interactions have on several specific determinants of long range organization: fluctuations, aggregation, phase separation, crystallization, and field-induced redistribution.

A. Fluctuations and Membrane Domains

On a thermodynamic scale, membrane systems are small, being limited in both spatial extent and number of constituent macromolecules. Thus, in membranes, fluctuation effects can be significant, and local properties can differ considerably from average properties. Here we focus on the relationship between fluctuations and domain formation, a relationship that has been well characterized for lipid systems (see Reference 54 and references therein). In particular, we show that fluctuations can lead to the creation of protein domains,

whose properties are determined by fluctuations in membrane composition and membrane curvature as well as by protein-protein interactions.

1. *Fluctuations in Membrane Composition*

The molecular coordinates shown in Figure 6 reveal that, even within a single-phase membrane of well-defined composition, there appear to exist relatively large protein domains characterized by different densities of protein. This type of long range organization arises when number density in the membrane is low; number fluctuations can then become large and the local density can differ markedly from the average density ρ. However, density fluctuations are influenced not just by average particle density but also very significantly by interactions between membrane components, as can be seen from the following simple physical arguments.

Consider an open region of membrane of area A, which proteins are free to enter and exit. On average, this region will contain $\langle N \rangle = \rho A$ molecules, where the brackets $\langle\ \rangle$ denote an ensemble average. However, the actual number of molecules within the region will fluctuate about this average. These fluctuations can be characterized by the variance in particle number, σ_N^2, which can be computed from the grand canonical partition function.[18,19,23,24] The result is[35]

$$\sigma_N^2 = \langle N^2 \rangle - \langle N \rangle^2 = \frac{k_BT\langle N \rangle}{(\partial\Pi / \partial\rho)_T} \qquad (20)$$

where Λ is the osmotic pressure, given by Equation 17, and $(\partial\Lambda/\partial\rho)_T$ is the isothermal osmotic compressibility. Note that since the dominant contribution to Λ can arise from the interaction dependent term in Equation 17, the variance, i.e., the magnitude of the fluctuations in particle number, can be markedly affected by interactions. In particular, repulsive protein-protein interactions will tend to reduce fluctuations and the size of domains, since repelling particles will tend to maximize distance from their neighbors. In contrast, attractive protein-protein interactions will tend to enhance fluctuations and the size of domains, since attracting particles will tend to aggregate. See Reference 35 for more details.

The domains created by fluctuations in protein density are dynamic and probably short lived (with a lifetime dictated by the appropriate diffusion coefficient). However, they may persist on a time scale that is significant for lipid diffusion and diffusion-controlled reactions. In addition, in a static picture of membrane protein organization, such as that obtained from electron microscopy, these domains may be misinterpreted as "permanent" membrane features.

2. *Fluctuations in Membrane Curvature (Undulations)*

It has been shown that fluctuations in protein concentration can give rise to a long range ordering of membrane proteins that is influenced by interactions. This is also true of fluctuations in membrane curvature, which lead to variations

or undulations in local membrane shape. When the membrane undulates, proteins can aggregate in regions of optimal membrane curvature or can be excluded from regions of inappropriate curvature. Moreover, membrane curvature can alter the way in which proteins interact and thereby further influence long range organization.

To make these ideas concrete, consider two specific examples. Spontaneous thermal fluctuations in the curvature of the erythrocyte membrane appear to induce the formation of glycoprotein-poor domains wherever membrane curvature is concave towards the extracellular space.[55] Such an ordering of the glycoprotein appears to arise because concave curvature forces extracellular sugar residues into atypically close proximity. This leads to strong repulsive interactions between the glycoproteins that are best minimized by their exclusion from concave regions of membrane.

Conversely, a long lived (age-related) curvature of the lens membrane appears to arise when the dominant protein of the lens membrane, MIP, aggregates into organized crystalline arrays. MIP arrays are located in concave regions of membrane and excluded from adjacent convex regions of membrane;[56–58] see Figure 12. Again this unusual organization is probably stabilized by interparticle interactions. Charged amino acid residues on MIP's extracellular domain are expected to interact repulsively with like-charged residues on MIP molecules in the very closely apposed membrane of the adjacent cell. Such a repulsive interaction would lead to the observed structural motif: a MIP-rich region in one cell membrane next to a MIP-poor region in a closely apposed membrane of an adjacent cell. MIP organization may be further stabilized by an attractive interaction between the protein and negatively charged lipids, which would cause excess lipid to accumulate in membrane regions in neighboring cells that are close to MIP-rich membrane.[58]

B. Protein Aggregation

Membrane proteins often are organized into sharply demarcated domains. For example, large-scale segregation of protein can arise if there are macroscopic changes in the properties of the membrane, such as a lateral phase separation or protein crystallization; such macroscopic segregation phenomena will be discussed later. In this section, we analyze segregation as it is manifest in the somewhat smaller-scale "aggregation" of membrane proteins. The discussion will focus on the role that protein-protein interactions play in determining the distribution of aggregate sizes and aggregate shapes.

Aggregation phenomena present unique problems when one is trying to understand how forces affect organization because all proteins cannot be treated equivalently. The inequivalence arises because proteins on the periphery of the aggregate experience forces that differ markedly from those experienced by proteins in the interior of the aggregate, since proteins on the periphery are missing neighbors on one side, while those in the interior are not. Consequently, new physical phenomena, such as edge tension, need to be considered when one

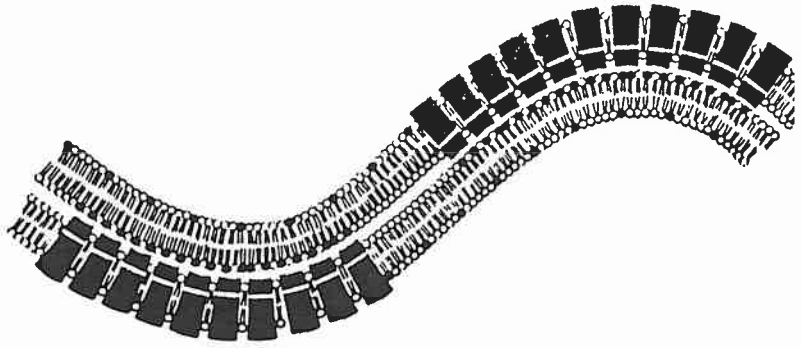

FIGURE 12. Relationship between membrane undulations and MIP protein organization in the len plasma membrane. MIP is segregated into large crystals in regions of the plasma membrane that ar concave toward the extracellular space and is excluded from adjacent convex regions of membran in the same cell and neighboring cells. It is thought that the curvature in the membrane is induce either by a protein cross section that is nonuniform and larger on the cytoplasmic side, or by protein protein interactions between charged amino acid residues. In addition, the alternating pattern of MI organization may be stabilized by an attractive lipid-protein interaction between positively charge amino acid residues on the protein and negatively charged lipids (black head groups) in th membrane of the adjacent cell. (From Zampighi, G. A., Hall, J. E., Ehring, G. R., and Simon, S. A *J. Cell Biol.*, 108, 2255, 1989. With permission.)

is analyzing the properties of an aggregate. One nice feature of aggregation an associated phenomena such as edge tension is that they are amenable to a flui theoretic analysis; in fact, it is possible to write the edge tension of the aggregat boundary as an integral over the interparticle force and radial distributio function (see Reference 59, and references therein). However, to date, aggrega tion in membranes has only been analyzed within the confines of thermodynami models and computer simulation methods. Confirmation of the predictions o these models must await further experimental work, which could be based o freeze-fracture electron microscopy or fluorescence energy transfer.[60]

Thermodynamic models have been used to analyze the role that protein protein interactions play in determining aggregate size, when monomers are i equilibrium with aggregates.[61,62] A Gibbs free energy function, which accounte for electrostatic repulsion between proteins within the aggregate, was con structed using relatively simple arguments. By minimizing the free energy, th dependence of the size and number of aggregates on edge tension, electrostati protein-protein interactions, and protein concentration was determined. Physi cally reasonable adjustment of these parameters led to the following results. A increase in either the electrostatic repulsion between proteins or in the edg tension of the aggregates reduced the fraction of particles that existed i aggregates and increased the fraction that existed as monomers. However increased electrostatic repulsions favored the formation of a relatively larg number of small aggregates, whereas increased edge tension favored the forma tion of a small number of large aggregates.

Monte Carlo simulation has been used to analyze the role that protein-protein interactions play in determining aggregate shape, when monomers bind irreversibly to aggregates.[63,64] The analyses always are based on some postulated aggregation mechanism, and two models of aggregation are frequently invoked: in "diffusion-limited aggregation" all monomers bind to a single, stationary aggregate, while in "cluster-cluster aggregation" the monomers bind to different mobile aggregates, and aggregates bind to other aggregates. Whichever model is invoked, if proteins always bind whenever they touch, loose stringy aggregates are formed. However, if proteins bind only a fraction of the time they touch, or if they always bind upon touching but can subsequently release and rebind, more compact aggregates are formed. See Figure 13.

C. Lateral Phase Separations

As mentioned previously, the long range organization of membrane proteins can be markedly altered by a change in the macroscopic state of the membrane, such as accompanies a phase transition. In keeping with the theme of this article, we address phase behavior by focusing on how membrane phase transitions and resulting phase structure (i.e., molecular organization) are influenced by protein-protein interactions.

A pure phospholipid bilayer containing only a single species of lipid undergoes an approximately first-order phase transition at some well-defined temperature, T_0; this transition temperature is determined largely by the nature of lipid-lipid interactions in the system. When protein molecules are added to the membrane, the phase behavior becomes more complex. The phase transition can take place over a broader temperature range, and the membrane can phase-separate into protein-rich and protein-poor domains. The more complex phase behavior of lipid-protein systems has its origins in lipid-protein and protein-protein interactions, as well as any protein-induced perturbations in lipid-lipid interactions.

Theoretical studies of interaction dependent phase behavior have focused primarily on describing effects arising from lipid-protein and lipid-mediated protein-protein interactions. The analyses have been based on phenomenological, thermodynamic models,[65-68] as well as more detailed statistical mechanical models and computer simulations.[69] Although direct protein-protein interactions have not been incorporated into these models, the qualitative effect of such interactions on membrane phase behavior seems intuitively clear. Attractive interactions should enhance the formation of protein-rich domains, while repulsive interactions should inhibit it.

Experimental studies have also been aimed at elucidating the role that lipid-protein and lipid-mediated protein-protein interactions play in determining phase behavior. In these studies, proteins were reconstituted into vesicles containing PCs of various acyl chain lengths. In such vesicles, bilayer thickness varies linearly with chain length.[70] Consequently, the vesicle system is well suited to simple manipulation of the match between hydrophobic and

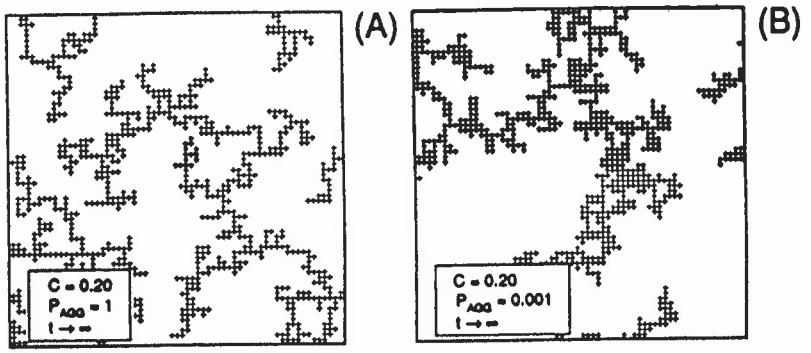

FIGURE 13. Influence of sticking probability on the final ($t \rightarrow \infty$) shape of cluster-cluster aggregates on a 64 × 64 square lattice. The probability of sticking per collision, P_{AGG}, is (A) 1 or (B) 0.001; the area fraction of proteins, C, is 20% for both membranes. Note that the cluster is more compact when $P_{AGG} = 0.001$ than when $P_{AGG} = 1$. Weaker sticking leads to more compact structures because proteins can penetrate farther into the cluster before final, irreversible binding occurs. (From Saxton, M. J., *Biophys. J.*, 61, 119, 1992. With permission.)

hydrophilic portions of the lipid and protein and any associated mismatch-induced lipid-protein or lipid-mediated protein-protein interaction.[21] The experiments demonstrated that the *in vitro* lateral distributions of rhodopsin,[43] BR,[43,71] and reaction center and antenna proteins from the photosynthetic apparatus of *Rps sphaeroides*[72,73] are sensitive to membrane thickness. Similar conclusions have emerged from studies of the *in vivo* distribution of proteins in the plasma membranes of *A. laidlawii*[47] and *Ustilago avenae*.[74]

The most obvious interpretation of these experimental results is that lipid-mediated protein-protein interactions influence distribution, although the results could also reflect thickness dependent changes in protein conformation. The strength and range of the lipid-mediated interactions deduced from the data show reasonable quantitative agreement with theoretical prediction, although at least some of the data suggest that the lipid-mediated protein-protein interaction is weaker than predicted by theory. Part of this disparity may reflect the fact that most theories of lipid-mediated interactions emphasize enthalpic contributions to the potential, while ignoring entropic contributions that will tend to randomize protein positions and so weaken the interaction. Recent theoretical work has taken entropic effects into account and has thereby improved the agreement between experiment and theory.[69]

D. Protein Crystallization

Another important macroscopic change in membrane state that fundamentally alters long range protein organization is protein crystallization. Crystalline order normally is thought of as something that is artificially induced during attempts to determine structure with diffraction techniques;[75] however, for

membrane systems, crystalline order can actually be found *in vivo*. For example, the membrane proteins BR, the ACHR, and the gap junction connexon are at least sometimes found to exist naturally in crystalline states in cell membranes.

Considerable effort has been directed at trying to identify the factors that lead to the crystallization of proteins. Although in many respects crystallization is a finicky, protein-specific process, it is now known to be quite generally affected by a number of variables, including protein concentration and the protein-protein force. Here we discuss results that illustrate the relationship between protein concentration, interprotein interactions, and membrane protein crystallization.

It is reasonable to expect that protein-protein forces will influence the formation of an ordered system such as a crystal, and, indeed, crystallization can sometimes be induced if the force is changed in an appropriate way. For example, under the influence of excluded-volume and electrostatic protein-protein interactions, gap junction connexons organize into dense, aggregated (but noncrystalline) plaques. However, if the protein-protein force is altered (presumably weakened) by adding cations such as calcium, which shield charge, the connexon proteins crystallize.[76]

Similarly, during attempts to crystallize membrane bound antibodies, it was noted that excluded-volume interactions can influence the size of the crystalline lattice.[77] This is manifest in the fact that as pH increases the lattice size grows. An increase in pH leads to greater antibody flexibility and a larger effective excluded-volume diameter; therefore, it was postulated that the observed increase in lattice size was associated with antibodies spreading apart due to a pH-induced increase in excluded-volume diameter.

Crystallization is also influenced by protein concentration. In fact, if the force is fixed and the protein concentration is raised sufficiently, a phase transition will take place that is accompanied by protein crystallization. This fact is exploited in crystallization protocols that rely on binding proteins to artificial membranes: as the proteins bind to the membrane they become more concentrated than they are in solution and crystallization becomes more likely.[78]

E. Field-Induced Redistribution of Proteins

We close our discussion of long range organization by showing that the effects of protein-protein interactions are also manifest when protein distribution is altered by applying an electric field to the membrane. External electric fields are commonly applied to membranes during postelectrophoresis relaxation experiments,[50] which are designed to measure diffusion coefficients. Moreover, endogenous fields can arise naturally during development or following injury, especially in epithelial tissues,[79] and could even lead to self-organization and pattern formation of charged channel proteins.[80–82]

Under the influence of the lateral force exerted by an external electric field, like-charged proteins will migrate towards one pole of a cell. This movement creates a nonuniform distribution of protein over the cell surface. The extent of the asymmetry in distribution is determined by many variables, but here we focus

primarily on our favorite, the protein-protein force. One would anticipate that i a nonideal system, repulsive interprotein forces would tend to reduce fiel induced asymmetry because, as the electric force acts to push like-charge proteins together at one side of a cell, repulsive interprotein interactions act a counteracting force that tends to push proteins apart. Indeed, such an effect wa observed when the distribution of the IgE receptor on rat basophilic leukemi cells was altered by a field.[83] The distribution of the receptor in a field wa reduced in asymmetry. The data could be satisfactorily fit to a model tha assumed the proteins experienced an external electric force and an excluded volume protein-protein force, but not to a model that assumed the protein experienced an external electric force alone;[83] see Figure 14.

VII. CONCLUSIONS

Two fundamental conclusions have emerged from the theoretical and experi mental work described in this paper. First, membrane proteins interact with thei neighbors. Second, these interactions are capable of profoundly affectin membrane organization and dynamics. In this section, we briefly review the mos salient aspects of our discussion and comment on the directions that future worl in this field should take.

Protein-protein interactions are ubiquitous in membranes: indeed, all mem brane proteins must interact, if only through excluded-volume forces. Experi ment shows that the "generic" protein-protein force is repulsive and probably ha its origin in short range excluded-volume forces and long range electrostati forces. However, in some cases the protein-protein force may also contain a lon range attractive component, which has its origin in protein-induced perturbatio of membrane lipids.

Protein-protein interactions have widespread effects on membrane proper ties. Over short distance scales (on the order of the average interparticle spacing) interactions lead to the creation of ordered but dynamic "coordination shells" around each protein. These shells are systematically observed in freeze-fracture electron micrographs of membranes, and they influence thermodynamic and transport properties of the membrane, as well as chemical reaction rates and energy transfer efficiencies. Fluid theory can be used to characterize the shells and to measure the protein-protein force. Over long distance scales, interactions affect phenomena as diverse as fluctuations in protein density, membrane phase behavior, and membrane protein crystallization.

Future work in this field should be directed toward at least three goals. First, experimental work should be directed at characterizing protein-protein interac tions more thoroughly, since the precise behavior of the membrane follows from the precise nature of the protein-protein force. Second, theoretical work should be directed at further exploring the connection between interactions and mem brane properties. For example, protein-protein forces affect protein mobility[14] as well as protein organization, and it is possible that other membrane properties

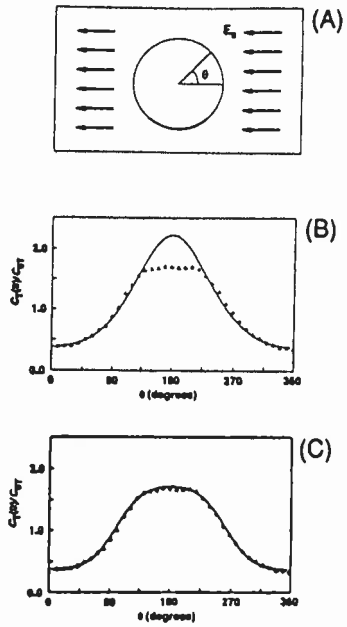

FIGURE 14. Influence of protein-protein interactions on the field-induced equilibrium distribution of IgE receptors on rat basophilic leukemia cells. (A) An electric field, E_0^*, of 15 V/cm was applied to the cells as indicated in the figure, and the relative surface concentration profile determined every 10 degrees over the cell surface. (B) The angular distribution of protein (triangles) is poorly fit to an ideal model (solid line) that neglects protein-protein interactions, particularly in regions of the cell where the applied field has induced the highest concentration of protein. (C) In contrast, the distribution is satisfactorily fit to a nonideal model (same definitions) that accounts for excluded-volume interactions between proteins. The effects of excluded-volume were modeled using Fermi-Dirac statistics. It should also be possible to describe the interaction-dependence of receptor distribution by equating the flux produced by the electric field with the flux produced by interaction-dependent mutual diffusion down the concentration gradient.[48] (Figure modified after Ryan, T. A., Myers, J., Holowka, D., Baird, B., and Webb, W. W., *Science*, 239, 61, 1988. With permission.)

are interaction dependent as well. Finally, the effects of molecular crowding and protein-protein forces on organization, dynamics, and function *in vivo* should be more thoroughly investigated.

ACKNOWLEDGMENTS

We are pleased to acknowledge helpful conversations on protein-protein interactions and protein organization with Joseph Costello, Ken Jacobson, and John Owicki. We are also indebted to Ken Jacobson and John Owicki for their useful comments on the manuscript and to Stephen Bicknese, Alan Verkman, and Daniel Zimet for their assistance with some of the figures.

APPENDIX: ALTERNATIVE CHARACTERIZATIONS OF PROTEIN ORGANIZATION

Thus far we have focused on studies of protein organization based on the prevailing (fluid-mosaic) model of biological membranes. In this model, the organization of proteins is dictated by protein-protein and lipid-protein interactions and can be understood using fluid theory, Monte Carlo simulation, and freeze-fracture electron microscopy. However, biological membranes have additional attributes that are not incorporated into the fluid-mosaic model, as is exemplified by protein attachment to an extramembranous skeleton. Therefore, methods not founded in fluid theory have also been used to characterize protein organization in biological membranes. The advantages and disadvantages of these alternative methods relative to the fluid-theoretic approach will be briefly discussed in this Appendix.

In some cases, the organization of proteins has been characterized by purely statistical methods (reviewed in Reference 84). Such studies do not seek to describe the mechanistic origins of protein organization, but rather seek simply to ascertain whether or not protein positions revealed in freeze-fracture electron micrographs are "random." A further goal of such work is to relate changes in the "randomness" of protein organization to changes in biological activity. An advantage of a simple statistical approach is that it is independent of an assumed model; a disadvantage is that it gives little, if any, insight into membrane behavior at the molecular level. In addition, the word random is simplistically used as a synonym for uniform. In fact, a distribution is random if it is described by an appropriate probability distribution, which can be distinctly nonuniform (see Figures 6 and 7).

In other cases, the organization of proteins has been characterized using simulation techniques based on nonequilibrium membrane models.[33,63,64,85-91] As was described in the text, classical Monte Carlo simulations are used to generate the distribution of molecules in thermally equilibrated, interacting fluids. In contrast, these alternative techniques are used to generate nonequilibrium distributions, such as those arising from random-sequential adsorption and immobilization, as well as various forms of aggregation mediated by strong contact attractions. Not surprisingly, equilibrium (Monte Carlo) and nonequilibrium membrane protein distributions differ markedly; see Figure 15. The nonequilibrium distributions will be valid in certain situations but will not describe protein organization in a truly fluid-mosaic membrane.

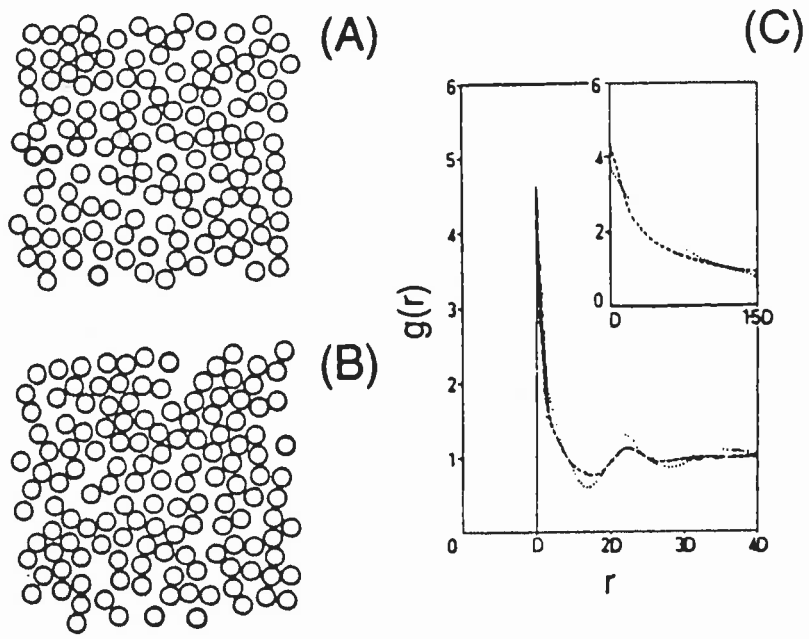

FIGURE 15. Comparison of Monte Carlo and other simulation algorithms. Particle configurations and radial distribution functions were generated for hard disks (excluded-volume interactions) occupying an area fraction $C = 0.5$. Monte Carlo simulations (A; dotted in C) model mobile, interacting particles at thermodynamic equilibrium. Random-sequential packing (B; dashed in C) models protein adsorption to the membrane followed by immediate immobilization. Detailed discussions of these and other simulation algorithms are given in Reference 90, and references therein. Note that the configurations and distribution functions shown in the figure differ, indicating that particle organization depends on the physical mechanisms generating the distribution. Also compare the discontinuous initial rise in $g(r)$ shown here for the hard disk system with the continuous initial rise in $g(r)$ shown in Figure 7 for the long range interactions. (After Cornell, B. A., Middlehurst, J., and Parker, N. S., *J. Colloid Interface Sci.*, 81, 280, 1981. With permission.)

REFERENCES

1. **Oliver, J. M. and Berlin, R. D.,** Mechanisms that regulate the structural and functional architecture of cell surfaces, *Int. Rev. Cytol.*, 74, 55, 1982.
2. **Sackmann, E.,** Physical basis of trigger processes and membrane structures, in *Biological Membranes*, Vol. 5, Chapman, D., Ed., Academic Press, London, 1984, 105.
3. **Gumbiner, B. and Louvard, D.,** Localized barriers in the plasma membrane: a common way to form domains, *Trends Biochem. Sci.*, 10, 435, 1985.
4. **Fraser, S. E. and Poo, M.-m.,** Development, maintenance, and modulation of patterned membrane topography: models based on the acetylcholine receptor, *Curr. Top. Dev. Biol.*, 17, 77, 1982.
5. **Steinbach, J. H. and Bloch, R. J.,** The distribution of acetylcholine receptors on vertebrate skeletal muscle cells, in *Receptors in Cellular Recognition and Developmental Processes*, Gorczynski, R. M., Ed., Academic Press, Orlando, FL, 1986, 183.
6. **Waxman, S. G. and Ritchie, J. M.,** Organization of ion channels in the myelinated nerve fiber, *Science*, 228, 1502, 1985.
7. **Sheetz, M. P.,** Membrane skeletal dynamics: role in modulation of red cell deformability, mobility of transmembrane proteins, and shape, *Semin. Hematol.*, 20, 175, 1983.
8. **Almers, W. and Stirling, C.,** Distribution of transport proteins over animal cell membranes, *J. Membr. Biol.*, 77, 169, 1984.
9. **Kell, D. B.,** Diffusion of protein complexes in prokaryotic membranes: fast, free, random or directed?, *Trends Biochem. Sci.*, 9, 86, 1984.
10. **Jacobson, K., Ishihara, A., and Inman, R.,** Lateral diffusion of proteins in membranes, *Annu. Rev. Physiol.*, 49, 163, 1987.
11. **Wolf, D. E.,** Overcoming random diffusion in polarized cells — corralling the drunken beggar, *BioEssays*, 6, 116, 1987.
12. **Tocanne, J.-F., Dupou-Cézanne, L., Lopez, A., and Tournier, J.-F.,** Lipid lateral diffusion and membrane organization, *FEBS Lett.*, 257, 10, 1989.
13. **Edidin, M.,** Molecular associations and membrane domains, *Curr. Topics Membr. Transp.*, 36, 81, 1990.
14. **Scalettar, B. A. and Abney, J. R.,** Molecular crowding and protein diffusion in biological membranes, *Comments Mol. Cell. Biophys.*, 7, 79, 1991.
15. **Ralston, G. B.,** Protein-protein interactions in cell membranes, in *Structure and Properties of Cell Membranes*, Vol. 1, Benga, G., Ed., CRC Press, Boca Raton, FL, 1985, 13.
16. **Abney, J. R. and Owicki, J. C.,** Theories of protein-lipid and protein-protein interactions in membranes, in *Progress in Protein-Lipid Interactions*, Vol. 1, Watts, A. and de Pont, J. J. H. H. M., Eds., Elsevier, Amsterdam, 1985, 1.
17. **Grasberger, B., Minton, A. P., DeLisi, C., and Metzger, H.,** Interaction between proteins localized in membranes, *Proc. Natl. Acad. Sci. U.S.A.*, 83, 6258, 1986.
18. **McQuarrie, D. A.,** *Statistical Mechanics*, Harper & Row, New York, 1976.
19. **Friedman, H. L.,** *A Course in Statistical Mechanics*, Prentice-Hall, Englewood Cliffs, 1985.
20. **Tsien, R. Y. and Hladky, S. B.,** Ion repulsion within membranes, *Biophys. J.*, 39, 49, 1982.
21. **Mouritsen, O. G. and Sperotto, M. M.,** Thermodynamics of lipid-protein interactions in lipid membranes: the hydrophobic matching condition, in *Thermodynamics of Membrane Receptors and Channels*, Jackson, M., Ed., CRC Press, Boca Raton, FL, 1992, chap. 4.
22. **Sperotto, M. M. and Mouritsen, O. G.,** Monte Carlo simulation studies of lipid order parameter profiles near integral membrane proteins, *Biophys. J.*, 59, 261, 1991.
23. **Hill, T. L.,** *Statistical Mechanics*, McGraw-Hill, New York, 1956.
24. **Chandler, D.,** *Introduction to Modern Statistical Mechanics*, Oxford University Press, New York, 1987.
25. **Singer, S. J. and Nicolson, G. L.,** The fluid mosaic model of the structure of cell membranes, *Science*, 175, 720, 1972.

26. **Braun, J., Abney, J. R., and Owicki, J. C.,** How a gap junction maintains its structure, *Nature*, 310, 316, 1984.
27. **Braun, J., Abney, J. R., and Owicki, J. C.,** Lateral interactions among membrane proteins: valid estimates based on freeze-fracture electron microscopy, *Biophys. J.*, 52, 427, 1987.
28. **Abney, J. R., Braun, J., and Owicki, J. C.,** Lateral interactions among membrane proteins: implications for the organization of gap junctions, *Biophys. J.*, 52, 441, 1987.
29. **Abney, J. R. and Owicki, J. C.,** An "exact" integral equation approach to the inverse problem in two-dimensional fluids, *Chem. Phys. Lett.*, 164, 73, 1989.
30. **Abney, J. R., Scalettar, B. A., and Owicki, J. C.,** Self diffusion of interacting membrane proteins, *Biophys. J.*, 55, 817, 1989.
31. **Abney, J. R.,** Protein-Protein Interactions in Membranes, Ph.D. thesis, University of California, Berkeley, 1987.
32. **Metropolis, N., Rosenbluth, A., Rosenbluth, M., Teller, A., and Teller, E.,** Equations of state calculations by fast computing machines, *J. Chem. Phys.*, 21, 1087, 1953.
33. **Jan, N., Lookman, T., and Pink, D. A.,** On computer simulation methods used to study models of two-component lipid bilayers, *Biochemistry*, 23, 3227, 1984.
34. **Mouritsen, O. G.,** Computer simulation of cooperative phenomena in lipid membranes, in *Molecular Description of Biological Membrane Components by Computer Aided Conformation Analysis*, Brasseur, R., Ed., CRC Press, Boca Raton, FL, 1990, 3.
35. **Abney, J. R., Scalettar, B. A., and Hackenbrock, C. R.,** On the measurement of particle number and mobility in nonideal solutions by fluorescence correlation spectroscopy, *Biophys. J.*, 58, 261, 1990.
36. **Chandler, D., Weeks, J. D., and Andersen, H. C.,** Van der Waals picture of liquids, solids, and phase transformations, *Science*, 220, 787, 1983.
37. **Widom, B.,** Intermolecular forces and the nature of the liquid state, *Science*, 157, 375, 1967.
38. **Hui, S. W., Ed.,** *Freeze-Fracture Studies of Membranes*, CRC Press, Boca Raton, FL, 1989.
39. **Markovics, J., Glass, L., and Maul, G. G.,** Pore patterns on nuclear membranes, *Exp. Cell Res.*, 85, 443, 1974.
40. **Gershon, N. D., Demsey, A., and Stackpole, C. W.,** Analysis of local order in the spatial distribution of cell surface molecular assemblies, *Exp. Cell Res.*, 122, 115, 1979.
41. **Stenberg, M. and Nygren, H.,** Long-range interactions in adsorbed layers of virus particles, *Phys. Rev. Lett.*, 59, 1164, 1987.
42. **Perelson, A. S.,** Spatial distribution of surface immunoglobulin on B lymphocytes: local ordering, *Exp. Cell Res.*, 112, 309, 1978.
43. **Pearson, L. T., Chan, S. I., Lewis, B. A., and Engelman, D. M.,** Pair distribution functions of bacteriorhodopsin and rhodopsin in model bilayers, *Biophys. J.*, 43, 167, 1983.
44. **Pearson, R. P., Hui, S. W., and Stewart, T. P.,** Correlative statistical analysis and computer modeling of intramembranous particle distributions in human erythrocyte membranes, *Biochim. Biophys. Acta*, 557, 265, 1979.
45. **Middlehurst, J. and Parker, N. S.,** Pair density distribution function of membrane particles at low density, *Biophys. J.*, 50, 1021, 1986.
46. **Baumann, G., Nonnenmacher, T. F., Frey, H., Melzner, I., and Haferkamp, O.,** Non-random spatial distribution of intermembraneous particles in red blood cell membrane, *Path. Res. Pract.*, 186, 159, 1990.
47. **Pearson, L. T., Edelman, J., and Chan, S. I.,** Statistical mechanics of lipid membranes: protein correlation functions and lipid ordering, *Biophys. J.*, 45, 863, 1984.
48. **Abney, J. R., Scalettar, B. A., and Owicki, J. C.,** Mutual diffusion of interacting membrane proteins, *Biophys. J.*, 56, 315, 1989.
49. **Scalettar, B. A., Abney, J. R., and Owicki, J. C.,** Theoretical comparison of the self diffusion and mutual diffusion of interacting membrane proteins, *Proc. Natl. Acad. Sci. U.S.A.*, 85, 6726, 1988.
50. **Young, S. H., McCloskey, M., and Poo, M.-m.,** Migration of cell surface receptors induced by extracellular electric fields: theory and applications, in *The Receptors*, Vol. 1, Conn, P. M., Ed., Academic Press, Orlando, FL, 1984, 511.

51. **Axelrod, D.,** Fluorescence photobleaching techniques and lateral diffusion, in *Spectroscopy and the Dynamics of Molecular Biological Systems*, Bayley, P. M. and Dale, R. E., Eds., Academic Press, London, 163, 1985.
52. **Petersen, N. O., Felder, S., and Elson, E. L.,** Measurement of lateral diffusion by fluorescence photobleaching recovery, in *Handbook of Experimental Immunology*, Vol. 1, Weir, D. M., Herzenberg, L. A., Blackwell, C., and Herzenberg, L. A., Eds., Blackwell Scientific, Palo Alto, CA, 24.1, 1986.
53. **Elson, E. L. and Qian, H.,** Interpretation of fluorescence correlation spectroscopy and photobleaching recovery in terms of molecular interactions, *Methods Cell Biol.*, 30, 307, 1989.
54. **Ipsen, J. H., Jørgensen, K., and Mouritsen, O. G.,** Density fluctuations in saturated phospholipid bilayers increase as the acyl-chain length decreases, *Biophys. J.*, 58, 1099, 1990.
55. **Zeman, K., Engelhard, H., and Sackmann, E.,** Bending undulations and elasticity of the erythrocyte membrane: effects of cell shape and membrane organization, *Eur. Biophys. J.*, 18, 203, 1990.
56. **Zampighi, G., Simon, S. A., Robertson, J. D., McIntosh, T. J., and Costello, M. J.,** On the structural organization of isolated bovine lens fiber junctions, *J. Cell Biol.*, 93, 175, 1982.
57. **Costello, M. J., McIntosh, T. J., and Robertson, J. D.,** Membrane specializations in mammalian lens fiber cells: distribution of square arrays, *Curr. Eye Res.*, 4, 1183, 1985.
58. **Zampighi, G. A., Hall, J. E., Ehring, G. R., and Simon, S. A.,** The structural organization and protein composition of lens fiber junctions, *J. Cell Biol.*, 108, 2255, 1989.
59. **Hill, T. L.,** *An Introduction to Statistical Thermodynamics*, Addison-Wesley, Reading, MA, 1960.
60. **Dewey, T. G. and Datta, M. M.,** Determination of the fractal dimension of membrane protein aggregates using fluorescence energy transfer, *Biophys. J.*, 56, 415, 1989.
61. **Gershon, N. D.,** Model for capping of membrane receptors based on boundary surface effects, *Proc. Natl. Acad. Sci. U.S.A.*, 75, 1357, 1978.
62. **Beretta, E. and Gambale, F.,** A thermodynamic interpretation to formation of clusters at the cell surface, *J. Theor. Biol.*, 108, 85, 1984.
63. **Finegold, L.,** Cell membrane fluidity: molecular modeling of particle aggregations seen in electron microscopy, *Biochim. Biophys. Acta*, 448, 393, 1976.
64. **Saxton, M. J.,** Lateral diffusion and aggregation: a Monte Carlo study, *Biophys. J.*, 61, 119, 1992.
65. **Abney, J. R. and Owicki, J. C.,** Phase diagrams for lipid bilayers containing intrinsic membrane proteins, *Biophys. J.*, 47, 494a, 1985.
66. **Mouritsen, O. G. and Bloom, M.,** Mattress model of lipid-protein interactions in membranes, *Biophys. J.*, 46, 141, 1984.
67. **Morrow, M. R. and Whitehead, J. P.,** A phenomenological model for lipid-protein bilayers with critical mixing, *Biochim. Biophys. Acta*, 941, 271, 1988.
68. **Sperotto, M. M., Ipsen, J. H., and Mouritsen, O. G.,** Theory of protein-induced lateral phase separation in lipid membranes, *Cell Biophys.*, 14, 79, 1989.
69. **Sperotto, M. M. and Mouritsen, O. G.,** Mean-field and Monte Carlo simulation studies of the lateral distribution of proteins in membranes, *Eur. Biophys. J.*, 19, 157, 1991.
70. **Lewis, B. A. and Engelman, D. M.,** Lipid bilayer thickness varies linearly with acyl chain length in fluid phosphatidylcholine vesicles, *J. Mol. Biol.*, 166, 211, 1983.
71. **Lewis, B. A. and Engelman, D. M.,** Bacteriorhodopsin remains dispersed in fluid phospholipid bilayers over a wide range of bilayer thicknesses, *J. Mol. Biol.*, 166, 203, 1983.
72. **Riegler, J. and Möhwald, H.,** Elastic interactions of photosynthetic reaction center proteins affecting phase transitions and protein distributions, *Biophys. J.*, 49, 1111, 1986.
73. **Peschke, J., Riegler, J., and Möhwald, H.,** Quantitative analysis of membrane distortions induced by mismatch of protein and lipid hydrophobic thickness, *Eur. Biophys. J.*, 14, 385, 1987.
74. **Hippe, S. and Lüth, H.,** A simple physical model for fungicide induced hexagonal clustering of intramembrane particles in the plasmalemma of *Ustilago avenae*, *J. Theor. Biol.*, 121, 351, 1986.

75. **Michel, H., Ed.,** *Crystallization of Membrane Proteins*, CRC Press, Boca Raton, FL, 1991.
76. **Peracchia, C.,** Calcium effects on gap junction structure and cell coupling, *Nature*, 271, 669, 1978.
77. **Uzgiris, E. E.,** Antibody organization on lipid films: influence of pH and interchain disulphide reduction, *Biochem. J.*, 272, 45, 1990.
78. **Uzgiris, E. E. and Kornberg, R. D.,** Two-dimensional crystallization technique for imaging macromolecules, with application to antigen-antibody-complement complexes, *Nature*, 301, 125, 1983.
79. **Robinson, K. R.,** The responses of cells to electrical fields: a review, *J. Cell Biol.*, 101, 2023, 1985.
80. **Fromherz, P.,** Self-organization of the fluid mosaic of charged channel proteins in membranes, *Proc. Natl. Acad. Sci. U.S.A.*, 85, 6353, 1988.
81. **Fromherz, P.,** Spatio-temporal patterns in the fluid-mosaic model of membranes, *Biochim. Biophys. Acta*, 944, 108, 1988.
82. **Fromherz, P.,** Self organization of a membrane in synaptic geometry, *Biochim. Biophys. Acta*, 986, 341, 1989.
83. **Ryan, T. A., Myers, J., Holowka, D., Baird, B., and Webb, W. W.,** Molecular crowding on the cell surface, *Science*, 239, 61, 1988.
84. **Hui, S. W.,** Analysis of irregular distributions and dynamics of membrane components by computer aided image recognition and statistical evaluation, in *Electron Microscopy of Subcellular Dynamics*, Plattner, H., Ed., CRC Press, Boca Raton, FL, 1989.
85. **Quickenden, T. I. and Tan, G. K.,** Random packing in two dimensions and the structure of monolayers, *J. Colloid Interface Sci.*, 48, 382, 1974.
86. **Dodds, J. A.,** Simplest statistical geometric model of the simplest version of the multicomponent random packing problem, *Nature*, 256, 187, 1975.
87. **Mason, G.,** Computer simulation of hard disc packings of varying packing density, *J. Colloid Interface Sci.*, 56, 483, 1976.
88. **Cornell, B. A., Chapman, D., and Peel, W. E.,** Random close-packed arrays of membrane components, *Chem. Phys. Lipids*, 23, 223, 1979.
89. **Finegold, L. and Donnell, J. T.,** Maximum density of random placing of membrane particles, *Nature*, 278, 443, 1979.
90. **Cornell, B. A., Middlehurst, J., and Parker, N.S.,** Modeling the simplest form of order in biological membranes, *J. Colloid Interface Sci.*, 81, 280, 1981.
91. **Freire, E. and Snyder, B.,** Quantitative characterization of the lateral distribution of membrane proteins within the lipid bilayer, *Biophys. J.*, 37, 617, 1982.
92. **Duniec, J. T., Goodchild, D. J., and Thorne, S. W.,** A method of estimating radial distribution function of protein particles in membranes from freeze-fracture electron micrographs, *Comput. Biol. Med.*, 12, 319, 1982.